DOE/FE/41220-13

MONITORING POWER PLANT EFFICIENCY USING THE MICROWAVE-EXCITED THERMAL-ACOUSTIC EFFECT TO MEASURE UNBURNED CARBON

Final Technical Progress Report

Reporting Period Start Date: September 1, 2001
Reporting Period End Date: December 31, 2004

Principal Author(s):
Robert C. Brown, Robert J. Weber, and Jeffrey J. Sweterlitsch

Date Report Issued:
January 2005

DOE Award Number:
DE-FC26-01NT41220

Submitted By:
Center for Sustainable Environmental Technologies
Iowa State University
285 Metals Development Bldg.
Ames, IA 50011-3020

DISCLAIMER

ABSTRACT

The objective of this project is to explore microwave-excited thermal-acoustic (META) phenomena for quantitative analysis of granular and powdered materials, with the culmination of the research to be an on-line carbon-in-ash monitor for coal-fired power plants. This technique of analyzing unburned carbon in fly ash could be a less tedious and time consuming method as compared to the traditional LOI manual procedure.

Phase 1 of the research focused on off-line single-frequency thermal-acoustic measurements where an off-line fly ash monitor was constructed that could operate as analytical tool to explore instrument and methodology parameters for quantifying the microwave-excited thermal-acoustic effect of carbon in fly ash, and it was determined that the off-line thermal-acoustic technique could predict the carbon content of a random collection of fly ashes with a linear correlation constant of $R^2 = 0.778$. Much higher correlations are expected for fly ashes generated from a single boiler. Phase 2 of the research developing a methodology to generate microwave spectra of various powders, including fly ash, coal, and inorganic minerals, and to determine if these microwave spectra could be used for chemical analyses. Although different minerals produced different responses, higher resolution microwave spectra would be required to be able to distinguish among minerals. Phase 3 of the research focused on the development of an on-line fly ash monitor that could be adapted to measure either a thermal-acoustic or thermal-elastic response to due microwave excitation of fly ash. The thermal-acoustic response was successfully employed for this purpose but the thermal-elastic response was too weak to yield a useful on-line device.

Keywords: fly ash, carbon monitor, unburned carbon, boiler instrumentation

EXECUTIVE SUMMARY

The objective of this project is to explore microwave-excited thermal-acoustic (META) phenomena for quantitative analysis of granular and powdered materials, with the culmination of the research to be an on-line carbon-in-ash monitor for coal-fired power plants. This technique of analyzing unburned carbon in fly ash could be a less tedious and time consuming method as compared to the traditional LOI manual procedure.

The research was divided into three phases. Phase 1 of the research focused on off-line single-frequency thermal-acoustic measurements where an off-line fly ash monitor was constructed that could operate as analytical tool to explore instrument and methodology parameters for quantifying the microwave-excited thermal-acoustic effect of carbon in fly ash. Phase 2 of the research involved modifying the off-line fly ash monitor so a range of microwave frequencies could be used to generate microwave spectra of fly ash, coal, and other powdered and granular materials for chemical analysis. Phase 3 of the research focused on the development of an on-line fly ash monitor that could be operated under either steady flowing conditions, or intermittent flowing conditions, would also be adapted to measure either thermal-acoustic waves with a microphone or thermal-elastic waves with an accelerometer.

The first phase research consisted of four specific objectives for using the single-frequency off-line fly ash monitor: identify appropriate parameters of the source of the microwaves; determine important experimental parameters with regard sample preparation; explore what role inorganic mineral matter in fly ash contributes to the thermal-acoustic response of the fly ash; and demonstrate how the single-frequency off-line thermal-acoustic fly ash monitor can predict the unburned carbon content in fly ash. It was determined that modulating the 1 GHz microwaves at a frequency of 20 Hz would produce the desired signal strength and the signal-to-noise ratio. Several experiments looked at sample compression and thermal-acoustic volume, and the research found that sample compression produced a stronger signal than an uncompressed sample, and the thermal-acoustic response was proportional to the inverse of the thermal-acoustic volume, but there were negligible effects on the thermal-acoustic response due to sample moisture, ambient moisture, and ambient temperature. It was found that the presence of silicon dioxide and iron (III) oxide can affect the linearity of the thermal-acoustic response, particularly when the unburned carbon content in the fly ash is less than 2%. Finally, the single-frequency off-line fly ash monitor was able to predict the unburned carbon content in fly ash with a linear correlation constant of $R^2 = 0.778$, covering the range of 2% – 18% carbon content. Much higher correlations are expected for fly ashes generated from a single boiler.

The second phase of the research consisted of generating microwave thermal-acoustic spectra of fly ash, coal, and inorganic mineral matter. It was determined that there are spectral differences among the different fly ashes, coal, and inorganic minerals, but improvements of the methodology for collecting and generating these spectra need to be made, including, but not limited to, increasing the resolution of the spectra and establishing a baseline spectrum.

The third phase of the research was to translate the technology of the single-frequency, off-line fly ash monitor, and construct an on-line version. The on-line version had the capability of measuring either a thermal-acoustic response or a thermal-elastic response of the fly ash. However, it was determined that only the thermal-acoustic method was able to predict the carbon content of the fly ash, with a linear correlation constant of $R^2 = 0.830$, whereas the thermal-elastic method was unsuccessful at predicting the carbon content in fly ash.

TABLE OF CONTENTS

INTRODUCTION

The traditional method for measuring carbon in ash, the loss-on-ignition (LOI) test, is a gravimetric technique: a sample heated at temperatures slightly above 100°C to drive off moisture, the sample is weighed and heated in an oxygen atmosphere to burn off carbon, and finally reweighed to determine the amount of carbon in a dry sample. This tedious and time consuming manual procedure requires 4 to 48 hours to perform and is subject to systematic errors in carbon determination.

Preliminary studies that suggest microwave-excited thermal-acoustic (META) spectroscopy has excellent potential as an analytical method for evaluating properties of powders. Microwave-excited thermal-acoustic spectroscopy is a relatively unexplored field, but it is based on two established technologies: microwave spectroscopy and the thermal-acoustic effect. The objective of this project is to explore microwave-excited thermal-acoustic (META) phenomena for quantitative analysis of granular and powdered materials, with the culmination of the research to be an on-line carbon-in-ash monitor for coal-fired power plants.

Phase 1 of the research focused on off-line single-frequency thermal-acoustic measurements. An off-line fly ash monitor was constructed that could operate as either a single microwave frequency analytical tool to explore what the instrument and methodology parameters are for quantifying the microwave-excited thermal-acoustic effect of carbon in fly ash, or a range of microwave frequencies could be used to generate microwave spectra.

Phase 2 of the research involved modifying the off-line fly ash monitor so a range of microwave frequencies could be used to generate microwave spectra of fly ash, coal, and other powdered and granular materials for chemical analysis. These spectra were examined to

determine if and how microwave thermal-acoustic spectroscopy could be used as an analytical tool for powders.

Phase 3 of the research focused on the development of an on-line fly ash monitor. An on-line version of the single-frequency, off-line thermal-acoustic fly ash monitor was constructed to examine the feasibility of conducting META measurements of flowing fly ash. The on-line fly ash monitor can be operated under either steady flowing conditions, or intermittent flowing conditions. The on-line fly ash monitor was also adapted to measure either thermal-acoustic waves with a microphone or thermal-elastic waves with an accelerometer.

BACKGROUND

The thermal-acoustic effect

The thermal-acoustic effect occurs when a solid, liquid, or gas absorbs modulated radiation and produces a periodic heating in the surrounding media. Density variations in the surrounding media as a result of this heating produce a minute acoustical wave that can be detected by a sensitive pressure transducer, such as a microphone [1].

Many theoretical models exist for the thermal-acoustic response of solid and condensed samples have developed theories on the subject [2-6]. Following the derivation of [2], the thermal-acoustic signal (PAS), q, is given by:

$$q = C \cdot \left(\frac{1}{\rho_s \cdot C_{p,s} \cdot k_s} \right)^{1/2} \cdot \left(\frac{(\beta \cdot \mu_s)^2}{(\beta \cdot \mu_s + 1)^2 + 1} \right)^{1/2} \quad \textbf{(1)}$$

while the phase, φ, of the signal is given by:

$$\varphi = \tan^{-1}\left(1 + \frac{2}{\beta \mu_s} \right) \quad \textbf{(2)}$$

with

$$C = \frac{I_0 \gamma P_0 k_g{}^{1/2}}{4 \lambda_g T_0 \pi f (\rho_g C_{p,g})^{1/2}} \quad \textbf{(3)}$$

and ρ is the density, C_p is the specific heat, k is the thermal conductivity, β is the optical absorption coefficient, μ is the thermal sampling depth, I_o is the incident radiation intensity, γ is the ratio of specific heats, P_o is the gas pressure, λ is the length of the cell, T_o is the gas temperature, and f is the modulation frequency of the radiation. The subscripts s and g denote properties of the solid and gas, respectively.

From **Equation 1**, the thermal-acoustic signal is expected to be proportional to the radiation intensity, inversely proportional to the cell volume and ambient temperature, and dependent on the thermo-physical properties of the sample and surrounding gas. It is also a strong function of the relationship between the thermal and optical properties of the sample and the modulation frequency.

The influences of both the optical absorption coefficient and the thermal sampling depth are crucial to understanding the advantages of microwave excitation of the thermal-acoustic effect. The sample's optical absorption coefficient, β, is a measure of the depth at which 63% of the incident radiation is absorbed in the sample. The thermal sampling depth, μ, is the depth from which the absorbed energy contributes 63% of the thermal-acoustic signal. It is related to the thermal-wave decay coefficient, a, by [7]:

$$\mu = \frac{1}{a} = \left(\frac{\alpha}{\pi f} \right)^{1/2} \qquad \textbf{(4)}$$

where the thermal diffusivity, α, is given by

$$\alpha = \frac{k}{\rho C_p} \qquad \textbf{(5)}$$

The strength of the thermal-acoustic signal is related to the amount of thermal energy that escapes the sample to generate a pressure wave at the surface of the sample. If the thermal sampling depth is less than the optical absorption depth, then the acoustical response will be proportional to the amount of optical energy absorbed within the thermal sampling depth. Thus, the signal will be proportional to the concentration of the absorbing material. However, as the absorption becomes stronger, the radiation does not penetrate as deeply into the sample. Eventually, the radiation is all absorbed within the thermal sampling depth; the entire radiation

incident on the sample contributes to the signal independent of the concentration of absorbing material. This condition is known as saturation.

The product of μ and β is useful in predicting the relationship between the thermal sampling depth and the optical absorption depth [6, 7]. If $\mu\beta << 1$, absorption is unsaturated, the response of the instrument is linear with concentration of the absorbent. Calibration of such an instrument is very simple and accurate. Absorption of infrared radiation, the usual excitation source for thermal-acoustic spectroscopy, is very strong in powders and frequently leads to saturation [7]. Previous work demonstrated saturation at relatively low concentrations in an instrument to measure unburned carbon in fly ash that was based on infrared thermal-acoustics [8]. With a thermal sampling depth of 28 μm and a comparable optical absorption depth ($1/\beta$) at about 8% carbon, saturation would be evident for many fly ashes. On the other hand, the optical absorption depth for microwaves in fly ash is on the order of 1 m even for 100% carbon and saturation is not a problem.

The thermal-elastic effect

An alternative method of quantifying the carbon content in the fly ash was proposed for the on-line fly ash monitor because the original design would have required a very specific and controlled air gap volume between the sensor and the fly ash, but creating and controlling such an air gap in a bed of flowing particles was thought not to be possible. Instead of detecting the thermal acoustic wave generated in a gas volume, the thermal elastic wave that is generated in the presence of microwave excitation would be detected. The thermal elastic wave arises from the periodic volume expansion of the bulk sample as a result of periodic heating (as opposed to

the production of an acoustic wave at the surface of the sample). The pressure, *P*, arising in the sample as a result of this thermal elastic wave is given by:

$$P = B\alpha_t\bar{\theta} \qquad \textbf{(6)}$$

where *B* is the bulk modulus of the solid sample, α_t is the coefficient of thermal expansion, and $\bar{\theta}$ is the average temperature rise in the sample. *B* was estimated to be 5 MPa from information available from the study of grains in hoppers and α_t was estimated to be 9 x 10^{-6} °C^{-1} from data on silica. The average temperature rise is calculated from an energy balance on the sample:

$$\bar{\theta} = \frac{I_0\left(1 - e^{-\beta\mu}\right)}{\rho C_p \mu A \varpi} \qquad \textbf{(7)}$$

where I_0 is the incident microwave power, β is the absorptivity of fly ash to microwave radiation, μ is the distance over which the microwaves are absorbed, ω is the modulation frequency, ρ is the density of the bulk powder, C_p is the heat capacity of the solid particles, and *A* is the cross-sectional area of irradiation.

For low absorptivity, which is inherent in the microwave-excited thermal-acoustic effect, **Equation 7** reduces to:

$$\bar{\theta} = \frac{I_0\beta}{\rho C_p A \varpi} \qquad \textbf{(8)}$$

Previous absorptivity experiments for fly ash found that 5 mW of power was absorbed for 1 W of incident microwave radiation for every 1% carbon content of the fly ash over a sample depth of 2.5 cm. Accordingly,

$$\beta = \frac{-ln\left(1 - I/I_0\right)}{\mu} \qquad \textbf{(9)}$$

This yields a value for β of 0.201 m^{-1}. Using this and the previous documented data in **Equation 8** yields an average temperature rise of 2.5 x 10^{-6} °C. Application of **Equation 6** indicates a pressure wave of magnitude 1.1 x 10^{-4} Pa through the sample. The acceleration, *a*, of the wall and the accelerometer attached to it is given by:

$$a = \frac{P \cdot A}{\left(m_t + \rho_w \cdot A \cdot t\right)} \qquad \textbf{(10)}$$

where m_t is the mass of the transducer, ρ_w is the density of the wall, and t is the thickness of the wall, which results in an approximate acceleration, *a*, of 3.9 μg. A sensitive accelerometer can have a response of as much as 1 V g^{-1}, resulting in a signal of 3.9 μV, which can be detected by a lock-in amplifier. **Appendix A** presents rigorous calculations used to predict the signal response for the specific equipment and specific fly ashes used in this research

Microwave spectroscopy

Microwave spectroscopy encompasses the electromagnetic spectrum from about 1 GHz to 1000 GHz. It is a well-developed science that is used to deduce the structure of a variety of chemical compounds [9]. In this respect, it compliments optical and infrared spectroscopy. However, microwave radiation offers unique capabilities for quantitative analysis of powders and granules: absorption of microwave radiation is independent of the size of the divided solids commonly processed by a variety of industries.

The total amount of radiation absorbed by a collection of particles is given by the integrated mass specific absorption coefficient [10]:

$$A_a = \int_0^\infty R_a(D)m(D) \Big/ \int_0^\infty m(D)dD \qquad \textbf{(11)}$$

where R_a is the single particle mass specific absorption coefficient ($m^2\ g^{-1}$) and $m(D)$ is the particle size mass distribution ($m\ g^{-1}$). In general, R_a is a complicated function of the permittivity and size of the particles. Unless the particle size distribution is unchanging with time, which is rarely the case in industrial processes, the integrated mass specific absorption coefficient A_a will depend on both mass concentration and size distribution of the particles. Under such circumstances, quantitative analysis of divided solid materials, such as powders, granules, or fibers, is extremely difficult. However, for radiation wavelength, λ, long compared to the diameter, D, of particles ($D/\lambda << 1$), Rayleigh scattering occurs, so R_a is independent of particle diameter [11]. For the particle size range of interest to many industries (D = 2 – 2000 μm), optical and infrared radiation (0.4μm < λ < 100 μm) are too short to achieve Rayleigh scattering. Microwave radiation, which ranges in wavelength from a few millimeters to tens of centimeters, is ideal for quantitative analysis of divided solid materials ranging from very fine fly ash to coarse particles of grain.

The quantity of microwave radiation absorbed will depend on the composition of the material and the dielectric properties of the constituents making up the material. The dielectric properties of materials can be described by its complex permittivity [12]:

$$\varepsilon = \varepsilon' - i\varepsilon'' \qquad \textbf{(12)}$$

where ε' is the dielectric constant and ε'' is the dielectric loss factor. The dielectric constant affects the wavelength of microwave radiation propagating through a dielectric material whereas the dielectric loss factor is indicative of the amount of microwave energy absorbed by the material and converted to heat. For a given material, these constants depend on the temperature of the material and the frequency of the microwave radiation that interrogates the material.

EXPERIMENTAL

Phase 1 – Single-Frequency Off-line Thermal-acoustic Experiments.

A single-frequency off-line fly ash monitor was constructed to develop the experimental methodology for determining the carbon content in fly ash, and to determine what sample handling factors may influence the repeatability of the thermal-acoustic measurements. **Figure 1** is a detailed schematic of the off-line fly ash monitor. The fly ash monitor consists of an aluminum test cell with a copper strip-line suspended in the center of the test cell where the microwaves were propagated into the test cell. A Teflon sample cup (that holds the fly ash sample) was mounted on a removable lid constructed out of aluminum and brass, and an ACO Pacific MK 224 1.3 cm Electret microphone mounted inside a microphone sleeve located within the same removable lid. The microphone is then secured to the base of the fly ash monitor by tightening the threaded compressor against the bearing shown in **Figure 1**.

Figure 2 is a photograph of the off-line monitor connected to the power supply and output signal of the microphone was connected to an ACO Pacific PS9200 pre-amplifier and power supply. The output signal from the pre-amplifier was connected to the data acquisition instrumentation.

Figure 3 is of the data acquisition instrumentation used for all experiments described in this final technical report. The equipment consists of a Protek 1825 dual DC power supply used by the microwave generation and control electronics, a BK Precision 4011 function generator that controls the amplitude modulation frequency of the microwaves, a computer-controlled Stanford Research Systems SR530 lock-in amplifier that reads the voltage output from the fly ash monitor, a BK Precision 212013 oscilloscope used to monitor the feedback control loop, and an aluminum utility box that contains a Mini-Circuits ZOS-1025 voltage controlled oscillator

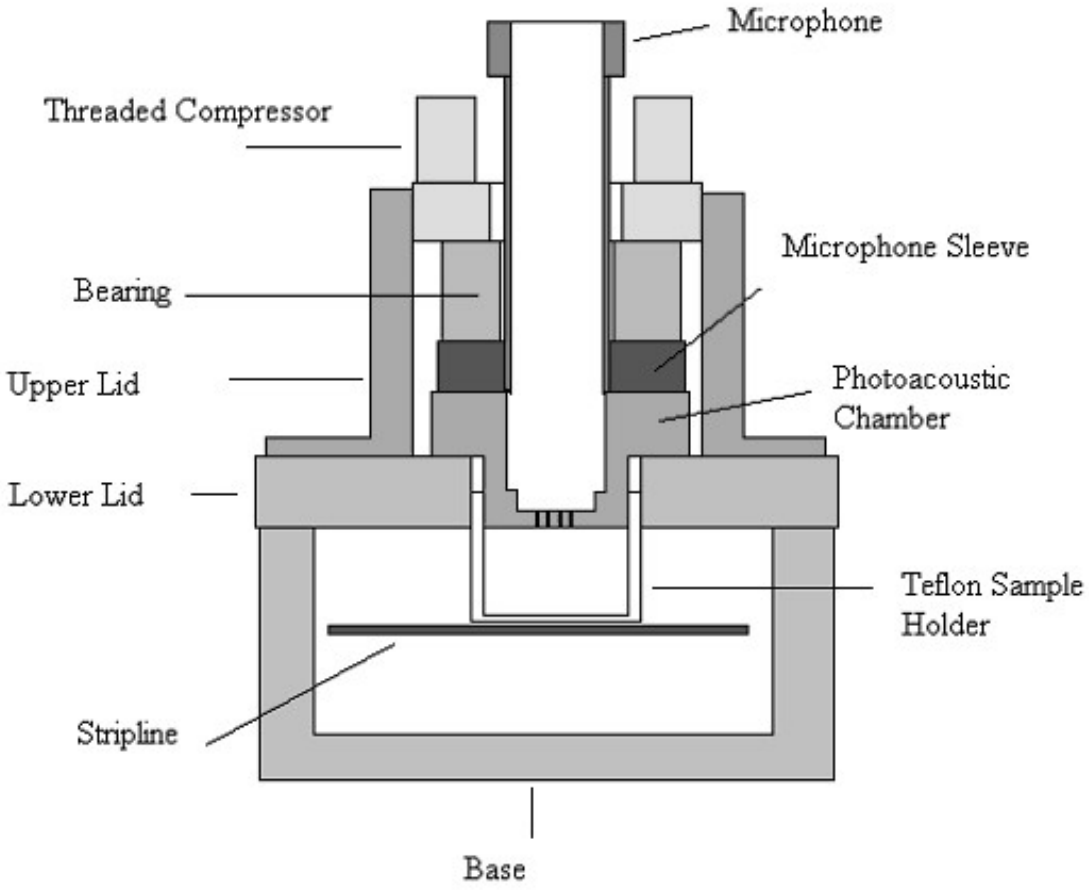

Figure 1. Cross-section schematic of the off-line fly ash monitor. Not to scale.

Figure 2. Off-line thermal-acoustic fly ash monitor.

Figure 3. Data acquisition cart showing DC power supply, function generator, lock-in amplifier, and other supporting equipment for generation and control of the microwaves used by the fly ash monitor.

that is the source of the microwaves, a Mini-Circuits ZSDR-425 Switch that modulates the microwaves, and additional electronic components used to filter and maintain the power level of the microwaves. Not shown in **Figure 3** is a Mini-Circuits LZY-2 microwave amplifier powered by a Topward 33010D DC power supply. **Schematic 1** of the **Appendix B** shows how this equipment was connected, including electronics contained within the aluminum utility box, and **Schematic 2** of **Appendix B** is of the control loop designed to stabilize the power level of the amplitude-modulated microwaves.

Phase 2 – Broadband Off-line Thermal-acoustic Spectrometer Experiments

Broadband off-line thermal-acoustic experiments were conducted in order to create microwave spectra of a variety of different chemicals, including fly ash samples, coal samples, and selected inorganic minerals. The original design was to generate microwave spectra of 1 – 10 GHz, but it was later determined that due to restraints imposed by the geometry of the off-line monitor, as well as a lack of the broadband microwave equipment required to generate, operate, and control microwaves of 1 – 10 GHz, it was decided to operate in a narrower bandwidth. A Hewlett-Packard 8648C Signal Generator was used to generate the variable microwave frequencies, which temporarily replaced the Mini-Circuits ZOS-1025 voltage controlled oscillator because the signal generator could generate the microwave with more control and ease.

A microwave thermal-acoustic spectrum was created by taking several measurements within the 500 – 1000 MHz range, and results were compiled into a single spectrum. Initial experiments were conducted with a low-power microwave amplifier which had a functional range of 500 – 2000 MHz, but a stronger signal response was desired, so the Mini-Circuits LZY-2 described in the previous section was used, however the functional range of this amplifier was

500 – 1000 MHz, so while the spectra generated by this high-power amplifier were much greater in magnitude, the bandwidth was reduced.

Phase 3 – Single-Frequency On-line Fly Ash Monitor Experiments

Figure 4 is a photograph of the on-line fly ash monitor system, including the support stands and feeders. At the top of the figure is a blue Tecweigh E/CR5 volumetric feeder with a stainless steel hopper mounted on a Uni-Strut support stand. A custom-designed variable-speed controller for this feeder is mounted on the right side panel. Attached to the end of the Tecweigh feeder is a plastic skirt that acts as a soft, flexible seal between the feeder and the top of the fly ash monitor. The fly ash monitor is mounted on an independent Uni-Strut stand to reduce the effect of mechanical vibrations from the two feeders on the fly ash monitor. Below the fly ash monitor is the bottom feeder, which is connected to the fly ash monitor with a second plastic skirt that acts as a soft, flexible seal. The customized hopper is made of clear acrylic so that the flow of the fly ash could be visually inspected. To improve the flow of the fly ash, a second shaft was ganged off the main shaft of the bottom feeder, and narrow spindles were attached to this second shaft that agitate and stir the fly ash, preventing it from bridging or compacting. The feeder tube is made of abrasion-resistant ultra-high molecular weight polyethylene (UHMW PE), which was selected because of its machinability. The feeder is powered by a Leeson 90VDC 44 W variable-speed motor controlled by a Baldor DC Drive controller with a maximum flow rate of 1 ft^3 hr^{-1}. The fly ash empties from the bottom feeder into a covered bucket to prevent fugitive dust emissions. The flow rate of the Tecweigh feeder can be adjusted to match the top speed of the bottom feeder, which is the desired flow rate of fly ash through the on-line monitor.

Figure 4. On-line fly ash monitor and supporting equipment.

Figure 5 is a mechanical drawing of the on-line fly ash monitor. The on-line fly ash monitor stands is 46.4 cm tall and is constructed out of aluminum. The fly ash monitor consists of four distinct regions: the control region; the freeboard region; the test region; and the exit region. The control region and test region are identical in shape except contained within the test region is the where the fly ash is exposed to the modulated microwaves during thermal-acoustic or thermal-elastic experiments. Baffles were installed in both the freeboard and exit regions to prevent the microwaves from escaping the test region. Only the test region was of importance for thermal-acoustic experiments, while thermal-elastic experiments were made at both the test and control regions.

Thermal-acoustic experiments

Figure 6 is a cross-section of the test region of the on-line fly ash monitor that shows the arrangement used for conducting thermal-acoustic experiments. Microwaves are introduced into the fly ash monitor by way of a copper strip line that was designed based on an approximation of the dielectric constant of fly ash, and has a characteristic impedance of 50 Ω at 1GHz. The copper strip was mounted on a Teflon block that is then fitted into the on-line fly ash monitor and both ends of copper strip were connected to N-type connectors (not shown). A Panasonic Omnidirectional Electret Condenser Microphone #WM-034CY195M was mounted inside a hollow stainless steel screw. On the surface of the microphone is a thin piece of felt that protects the internal electronics of the microphone; inherent in the design of the microphone is a narrow gap where the thermal-acoustic wave is generated and detected by the microphone's internal electronics. The set screw was used to precisely align the felt surface of the microphone with the fly ash in the monitor. The set screw was installed an aluminum mounting bracket that was secured to the front of the fly ash monitor.

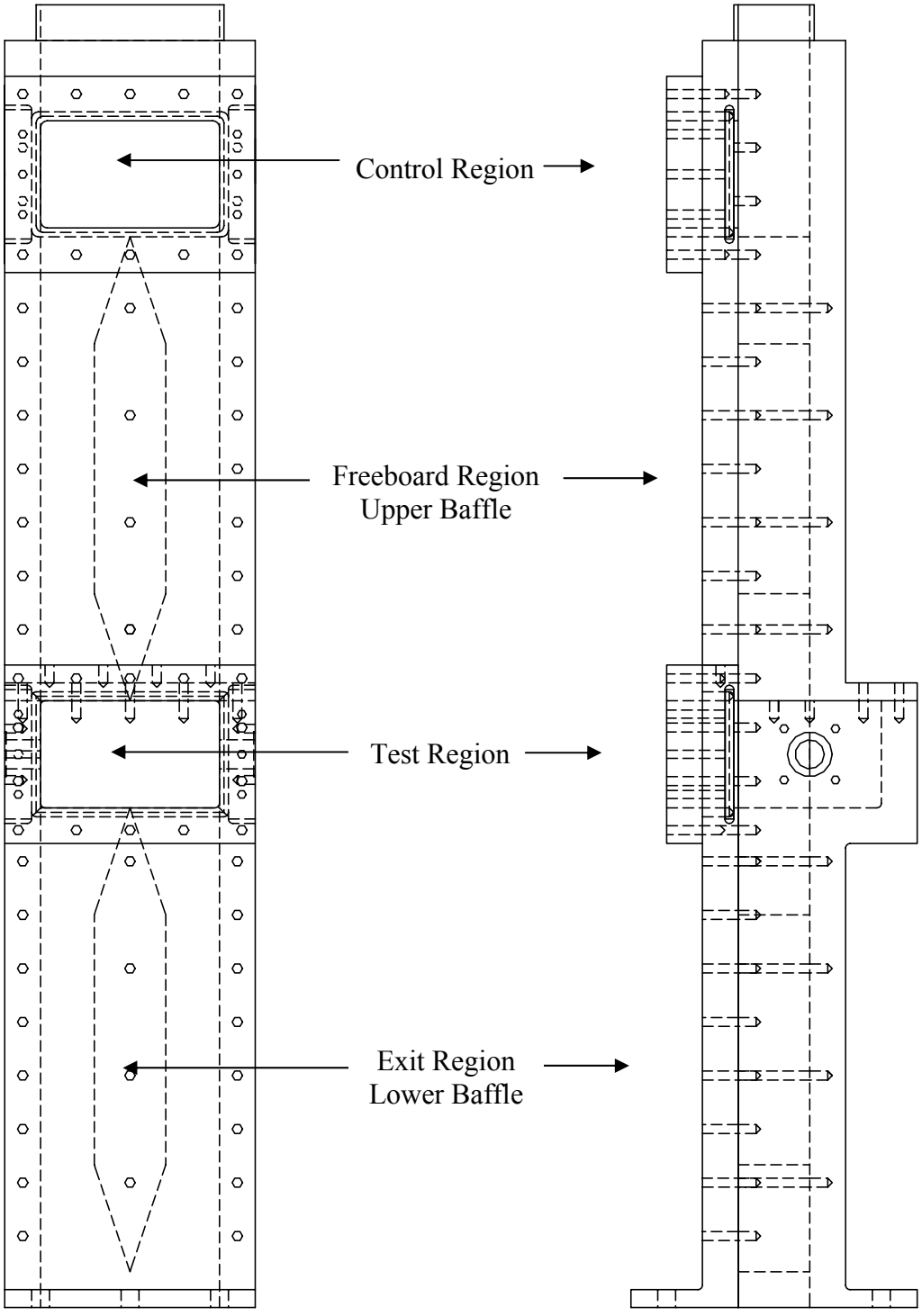

Figure 5. Mechanical drawings of the on-line fly ash monitor showing control region, test region, and the arrangement of the baffles. The left image is the front view, the right images is a side view. Not shown is the microphone for thermal-acoustic experiments or the accelerometers for thermal-elastic experiments, as well as all electrical cables. Scale is approximately 1:3.

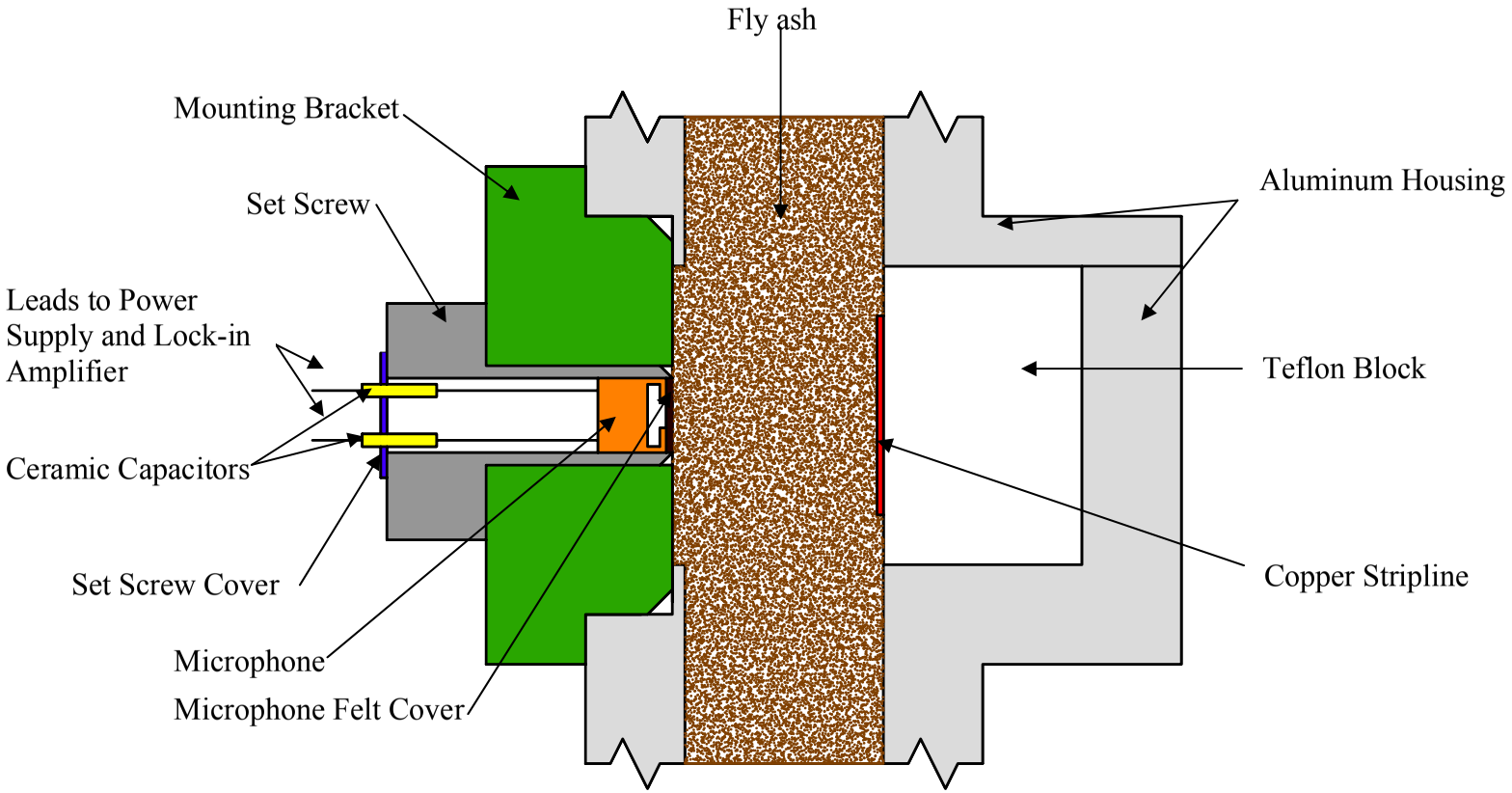

Figure 6. Cross-section schematic of the on-line fly ash monitor for thermal-acoustic experiments. Not to scale.

The leads from the microphone were connected to ceramic capacitors that were soldered to a thin sheet of metal (the set screw cover). The capacitors sole purpose was to provide electrical insulation between the all-metallic body of the fly ash monitor and the lead wires of the microphone.

Figure 7 is a photograph showing how the microphone assembly, described for **Figure 6**, was installed on the on-line fly ash monitor. The small circuit board in the middle of the figure is of bias circuitry that provides both the power supply for the microphone as well as the signal output from the microphone to the lock-in amplifier. A battery power supply (not shown) was selected because it is more stable than a DC power supply, which could have minute power level oscillations. **Schematic 3** of **Appendix B** provides the details of the bias circuitry.

Thermal-elastic experiments

Figure 8 is a cross-section of the test region of the on-line fly ash monitor that shows the arrangement used for conducting thermal-elastic experiments. Again, microwaves are introduced into the fly ash monitor by way of a copper strip line mounted on a Teflon block. An Applied MEMS SF1500-L Low-Noise accelerometer is mounted on a 51 μm-thick aluminum diaphragm using double-sided Kapton® Tape, which also acts as a dielectric to protect the sensitive electronics of the accelerometer.

The diaphragm is secured to the aluminum housing of the fly ash monitor with a mounting bracket of a different design than for the one used for thermal-acoustic experiments. Not shown are two small clamps and adjustable set screws that slightly stretch the diaphragm, thereby making the diaphragm more sensitive to vibrations caused by the thermal-elastic waves that would propagate through the fly ash.

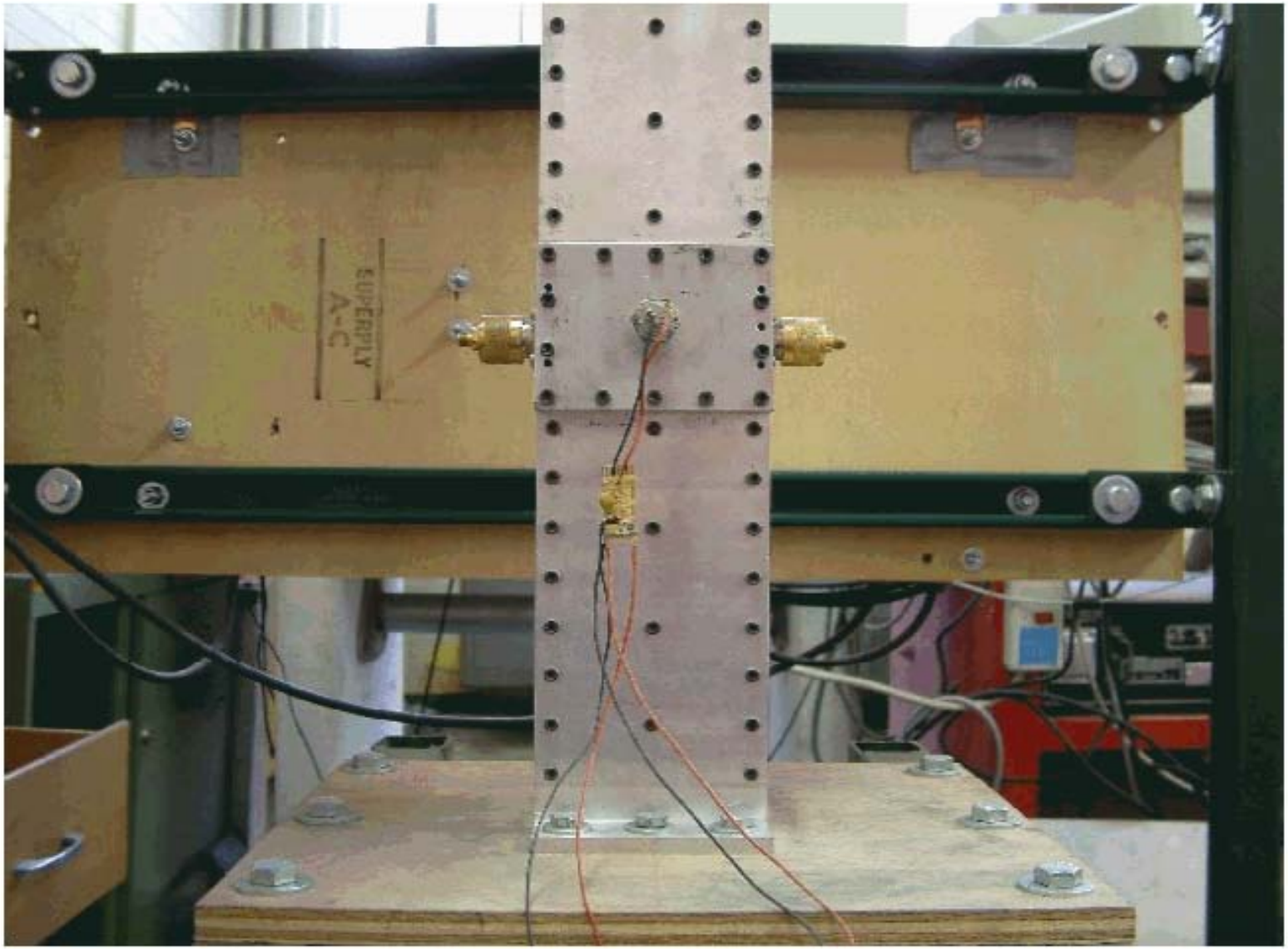

Figure 7. On-line fly ash monitor with microphone and bias circuitry for thermal-acoustic measurements.

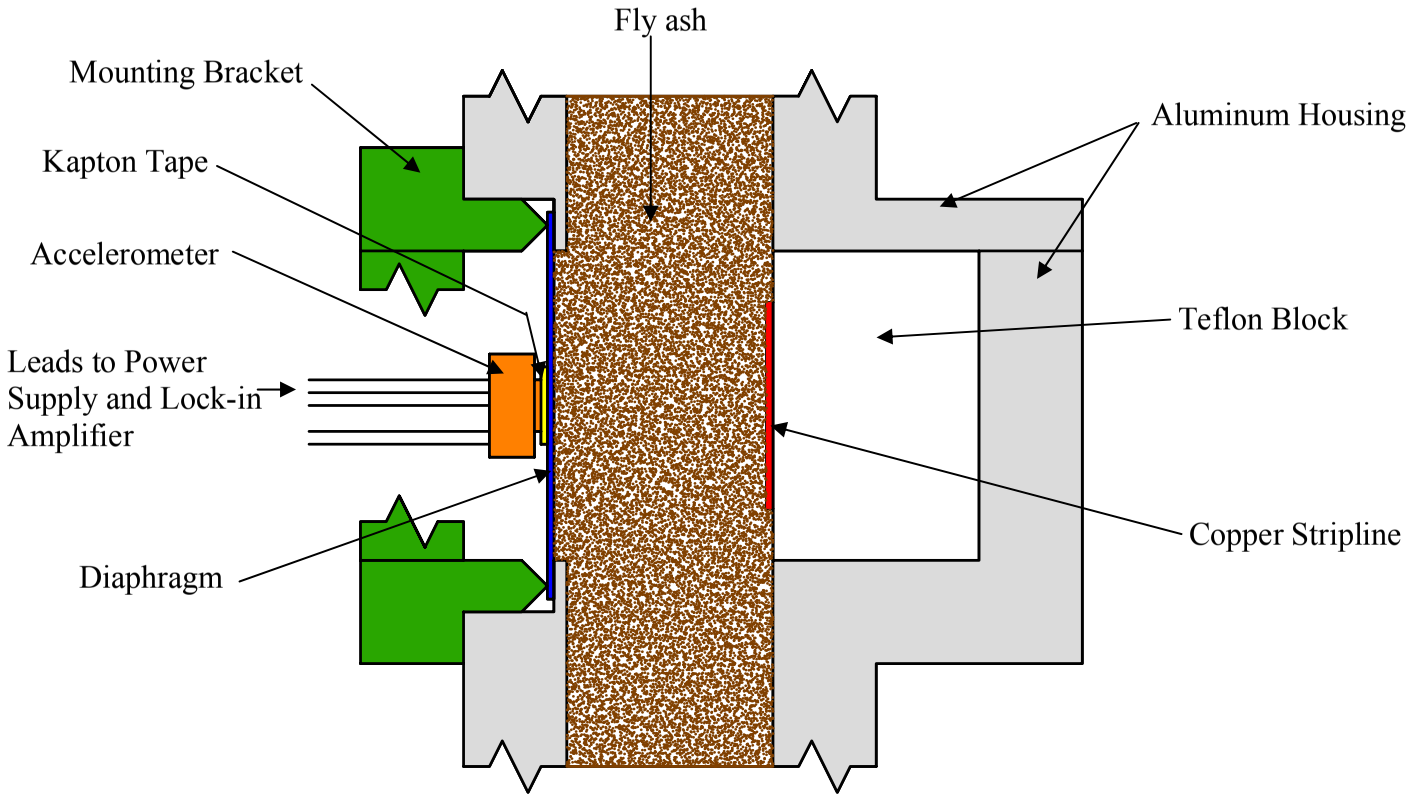

Figure 8. Cross-section schematic of on-line fly ash monitor for thermal-elastic measurements. Not to scale.

Figure 9 is of the on-line fly ash monitor showing the dual-accelerometer / dual-diaphragm arrangement with the battery-powered active noise control circuitry. The electrical box in the middle of the figure contains the power supply (two 9 V batteries) for the accelerometers, as well as the instrumentation-quality differential operational-amplifier circuitry. Toggle switches allow the user to control whether the desired signal comes from an individual accelerometer or from the differential op-amp. The test accelerometer is mounted below the electrical box, and the control accelerometer is mounted above the electrical box. The control accelerometer is mounted on the fly ash monitor in the same manner as the test accelerometer, and is also located sufficiently far enough away so that the microwaves do not induce a thermal-elastic effect in the fly ash in the vicinity of the second accelerometer: only the test accelerometer is subject to the microwave-induced thermal-elastic waves of the fly ash. The signal outputs from both accelerometers are fed into an instrumentation-quality differential operational-amplifier, which is designed to cancel out all signals except those at the amplitude modulation frequency of the microwaves.

The individual responses of the accelerometers are not identical. The test accelerometer has a response of 1.171 V g^{-1}, while the control accelerometer has a response of 1.136 V g^{-1}. The differential op-amp was designed to incorporate two potentiometers that can be used to adjust the gain for each accelerometer to account for the difference in response. The goal was to obtain an overall gain close to 2. **Schematic 4** of **Appendix B** is of the differential op-amp circuitry.

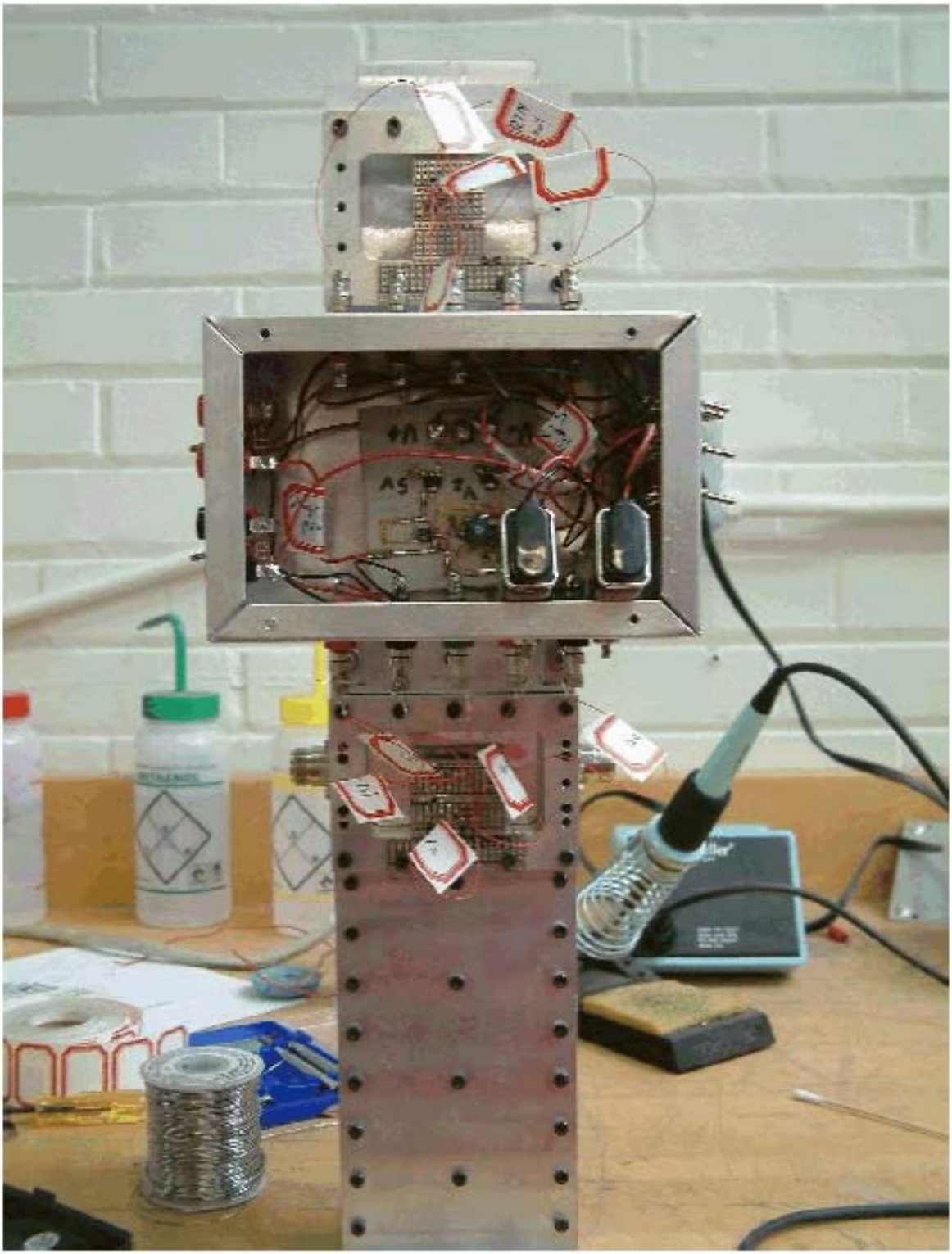

Figure 9. On-line fly ash monitor with dual diaphragms, dual accelerometers, and the electronics used for power the accelerometers as well as the active noise control electronics.

RESULTS AND DISCUSSION

Phase 1 – Single-Frequency Off-line Thermal-acoustic Fly Ash Monitor

The first phase of the research was to identify operational parameters of the off-line thermal-acoustic fly ash monitor, to develop a methodology of performing the thermal-acoustic measurements, and to determine the feasibility of using a single-frequency microwave to induce a thermal-acoustic effect in fly ash that would be proportional to the unburned carbon content in the fly ash. Once established, the operational parameters and method was to be translated from a single-frequency monitor to a broad-band spectrometer to determine if microwave spectra could be generated and if spectral features could be used to identify individual species in fly ash. Finally, an on-line version of the original single-frequency, off-line fly ash monitor would be constructed and tested to establish the feasibility of performing on-line thermal-acoustic measurements of fly ash.

The four major objectives for using the single-frequency off-line fly ash monitor were: 1) establish the amplitude modulation frequency of 1 GHz microwaves that produce the best thermal-acoustic response in the fly ash while maintaining a high signal-to-noise ratio; 2) determine what experimental parameters with regard to individual sample preparation and the laboratory environment would influence the repeatability and linearity of the thermal-acoustic measurements of the fly ash; 3) explore whether inorganic mineral matter in the fly ash may contribute to the overall thermal-acoustic response of the fly ash; and 4) demonstrate how the single-frequency off-line thermal-acoustic fly ash monitor can predict the unburned carbon content in fly ash.

The first objective was to establish the amplitude modulation frequency of 1 GHz microwaves that produce the best thermal-acoustic response in the fly ash while maintaining a

high signal-to-noise ratio. Fly ash from Prairie Creek Station, IA (3.77% carbon content based on LOI measurements) was used for this experiment. The modulation frequency was varied from 4 – 44 Hz. The thermal-acoustic response of the fly ash was then compared with the thermal-acoustic response of KBr, which is known to be transparent to microwave energy and therefore any thermal-acoustic response would be due to instrument noise. **Figure 10** shows the thermal-acoustic response of the fly ash, the KBr, and the signal-to-noise ratio. As predicted by theory, the strength of the thermal-acoustic response was inversely proportional to the amplitude modulation frequency of the microwaves; however, the best signal-to-noise ratio occurred at modulation frequencies of 8 – 22 Hz, so 20 Hz was selected as the modulation frequency for all subsequent thermal-acoustic measurements of the research, including Phase 2 and Phase 3 thermal-acoustic measurements.

The second objective was to determine what experimental parameters with regard to individual sample preparation and the laboratory environment would influence the repeatability and linearity of the thermal-acoustic measurements of the fly ash. Sample 223360AT from Duquesne/Elrama 3B, PA, (7.30% carbon content based on LOI measurements) was used for heterogeneity, compression, thermal-acoustic volume experiments, and sample moisture, and fly ash containing 15.19% carbon content based on LOI measurements was used for ambient humidity and temperature experiments.

The effect of sample heterogeneity was determined by measuring 3.12 gm of 22360AT fly ash and measuring the thermal-acoustic response of the fly ash, and then repeating the procedure with additional quantities of the same fly ash so that a total of 10 measurements were made on the same fly ash, referred to as “Test IA”. This entire procedure was repeated several days later, referred to as “Test IIA”, and a Student’s T-Test using Microsoft Excel was

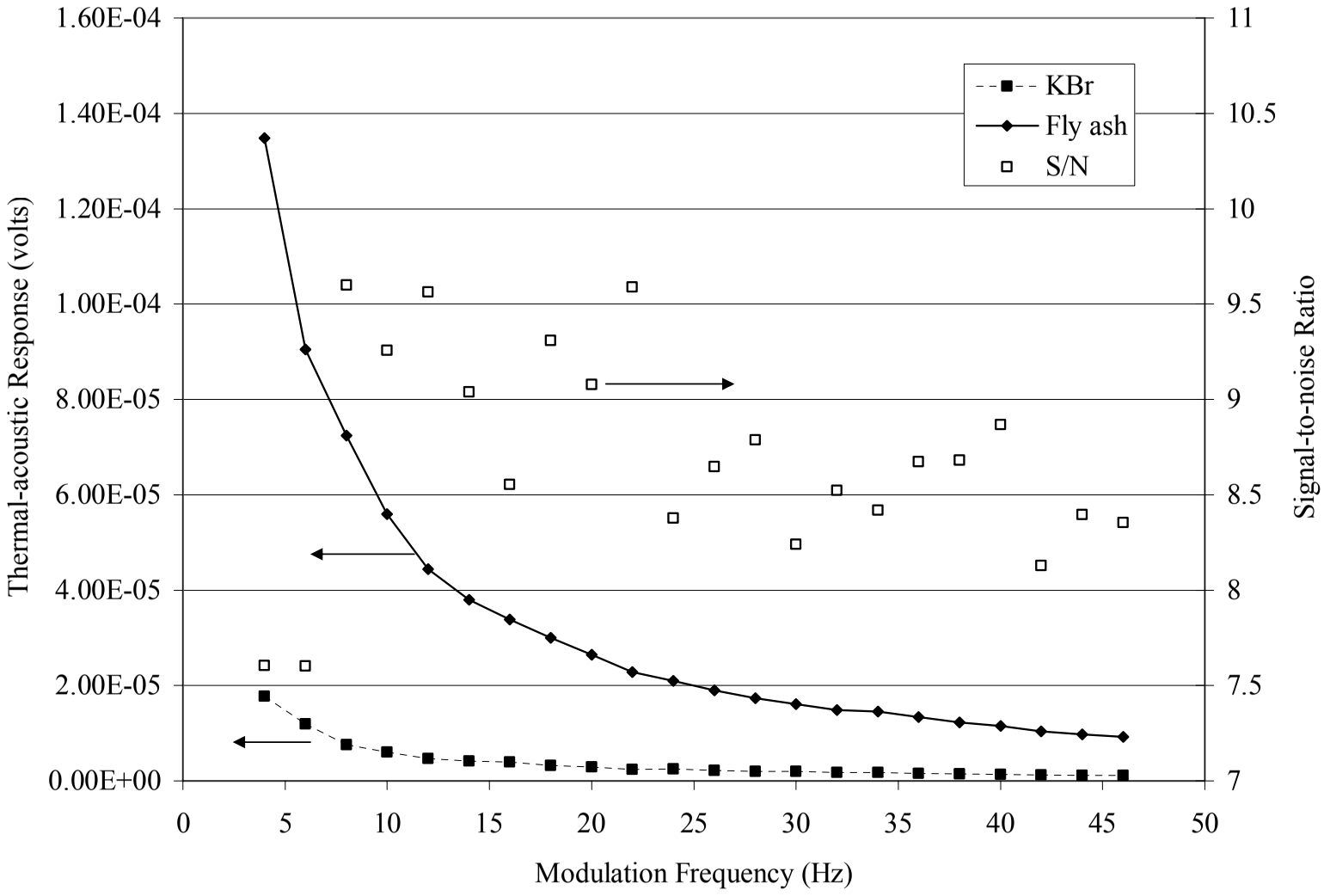

Figure 10. Thermal-acoustic response of fly ash and signal-to-noise ratio of the thermal-acoustic response at different amplitude modulation frequencies of 1 GHz microwaves.

conducted on the data to determine if the fly ash was sufficiently homogeneous. **Table 1** shows that the t-statistic is less than both the t-Critical one-tail statistic and the t-Critical two-tail statistic, therefore there is no statistical difference between the average thermal-acoustic responses for the fly ash due to poor homogeneity of fly ash material.

The effect of compressing the sample was determined by measuring 3.12 gm of 22360AT fly ash, and when the fly ash was in the sample cup a 2 kg brass piston was placed on top of the fly ash, compressing the fly ash, after which the thermal-acoustic response of the fly ash was measured. This procedure was repeated for a total of 10 measurements. This thermal-acoustic data, referred to as "Test III", was then compared with the data from "Test IA", and a Student's T-Test using Microsoft Excel was conducted data to determine how compressing the fly ash sample influences the thermal-acoustic response. **Table 2** shows that the absolute value of the t-statistic is greater than both the t-Critical one-tail statistic and the t-Critical two-tail statistic, therefore compressing the fly ash has a statistically significant effect on the thermal-acoustic response of the fly ash; all subsequent samples (fly ash, coal, or mineral matter) that were measured using the off-line fly ash monitor were compressed because **Table 2** indicates that compressing the sample increases the thermal-acoustic response.

Table 1. Microsoft Excel Student's T-Test analysis assuming equal variances that was used to determine if there is a statistical difference in signal due to sample heterogeneity.

	Test IA (thermal-acoustic)	Test IIA (thermal-acoustic)
Mean (Volts)	5.476×10^{-5}	5.329×10^{-5}
Variance	3.218×10^{-11}	2.231×10^{-11}
Observations	10	10
Pooled Variance	2.723×10^{-11}	
Expected Mean Difference	**0**	
df	18	
t Stat	**0.630**	
P (T<=t) one-tail	0.268	
t Critical one-tail	**1.734**	
P (T<=t) two tail	0.536	
t Critical two-tail	**2.101**	

The influences of the laboratory's ambient relative humidity and temperature on the thermal-acoustic response were tested over a six-month period. The extended time period was necessary because environmental control of the laboratory was limited: experiments were conducted from January through June where the relative humidity varied from 10 – 57%, and the temperature varied from 24 – 30 °C. A total of 18 measurements were made using fly ash that contained 15.19% carbon content during this time period, and linear regression analysis was performed to determine if there was any variation of the thermal-acoustic response due to changes in ambient relative humidity or ambient temperature. **Table 3** presents the results of the Microsoft Excel regression analyses for ambient relative humidity and ambient temperature.

Table 2. Microsoft Excel Student's T-Test analysis assuming equal variances that was used to determine how compressing the fly ash sample influences the thermal-acoustic response.

	Test IA (thermal-acoustic)	Test IIIA (thermal-acoustic)
Mean (Volts)	5.476×10^{-5}	6.182×10^{-5}
Variance	3.218×10^{-11}	4.503×10^{-11}
Observations	10	10
Pooled Variance	3.859×10^{-11}	
Expected Mean Difference	**0**	
df	18	
t Stat	**-2.541**	
P (T<=t) one-tail	0.010	
t Critical one-tail	**1.734**	
P (T<=t) two tail	0.020	
t Critical two-tail	**2.101**	

Table 3. Microsoft Excel Regression analyses to determine how the thermal-acoustic response of fly ash is influences by ambient relative humidity, ambient temperature, and sample moisture content.

	Ambient Relative Humidity	Ambient Temperature	Sample Moisture Content
Fly ash sample	15.19% carbon fly ash	15.19% carbon fly ash	#22360AT (see **App. C**)
Multiple R	8.536×10^{-3}	0.541	0.167
R – square	**7.286×10^{-5}**	**0.293**	**0.0280**
Adjusted R–square	-0.0624	0.249	-0.296
Standard Error	4.506×10^{-6}	3.789×10^{-6}	1.040×10^{-5}
Observations	**18**	**18**	**5**

The very low R^2 values for both regression analyses demonstrate that variations in ambient relative humidity and ambient temperature do not have a statistically significant impact on the repeatability of the off-line thermal-acoustic measurements of fly ash. Thus, the instrument is robust to changes in temperature and humidity.

Table 3 also presents regression analysis on 22360AT fly ash for five different moisture contents, ranging from 0.0 – 0.9% (by mass). To prepare fly ash samples of different moisture contents, one quantity of fly ash was dried in an oven at 110 °C for eight hours to complete remove any traces of moisture (referred to as "dry"), while a second quantity of the same fly ash was placed in a water-filled desiccator for twenty-four hours to allow the fly ash to absorb water vapor (referred to as "wet"). Three fly ash mixtures were made from these dry and wet fly ashes such that the wet:dry mass ratios of the fly ash mixtures were 3:1, 1:1, and 1:3. These mixtures, along with the original wet and dry samples, where then analyzed in the off-line monitor. The moisture content of the wet fly ash determined by weighing a sample of the wet fly ash, then the fly ash was heated in an oven at 110 °C for eight hours, and the fly ash was re-weighed to determine the amount of moisture that evaporated from the fly ash. As evident in **Table 3**, the low R^2 value indicates that sample moisture in the tested range did not statistically affect the thermal-acoustic response. It should be noted, however, that the range of moisture contents, 0.0 – 0.9%, is rather narrow but appropriate to fresh fly ash samples extracted from a boiler.

To determine how the thermal-acoustic volume (the air gap between the surface of the powder sample and the microphone) affects the thermal-acoustic response of the fly ash, nine measurements were made on 22360AT fly ash. For the first measurement, the sample cup of the off-line fly ash monitor was filled with fly ash, the fly ash was then compressed, and the height of the sample was measured, after which the thermal-acoustic measurement was made on

the fly ash. When the thermal-acoustic measurement was finished, a small amount of fly ash was removed from the sample cup, and the compression, sample height measurement, and thermal-acoustic measurement procedures were repeated for a total of nine different sample heights. From these sample heights the air gap volumes were calculated, and the thermal-acoustic response for each measurement was compared with the reciprocal of the air gap volume, because, according to thermal-acoustic theory and **Equations 1 – 3**, the thermal-acoustic response is proportional to the inverse of the cell length. The data in **Figure 11** reinforce this theory.

To summarize the results of the second objective for evaluating the single-frequency off-line thermal-acoustic fly ash monitor: the thermal-acoustic response of fly ash is independent of the sample heterogeneity, sample moisture content, and ambient humidity and temperature variations; compressing the fly ash increases the thermal-acoustic response of the fly ash; and the thermal-acoustic response is dependent on the air gap volume between the surface of the powder sample and the microphone. For subsequent off-line thermal-acoustic measurements, the powdered samples were compressed, and the air gap volume was controlled.

The linear relationship between the reciprocal of the thermal-acoustic air gap volume and the thermal-acoustic response introduces the capability of mathematically scaling the thermal-acoustic response to a specific air gap volume, as described by **Equation 13**:

$$\frac{PA_{raw} \cdot gap\ volume_{measured}}{gap\ volume_{specified}} = PA_{gap-compensated} \qquad \textbf{(13)}$$

where PA_{raw} is the measured thermal-acoustic response, $gap\ volume_{measured}$ is the calculated air gap volume based on sample height measurements, $gap\ volume_{specified}$ is a user-specified air gap volume, and $PA_{gap\text{-}compensated}$ is the gap-compensated thermal-acoustic response of the fly ash.

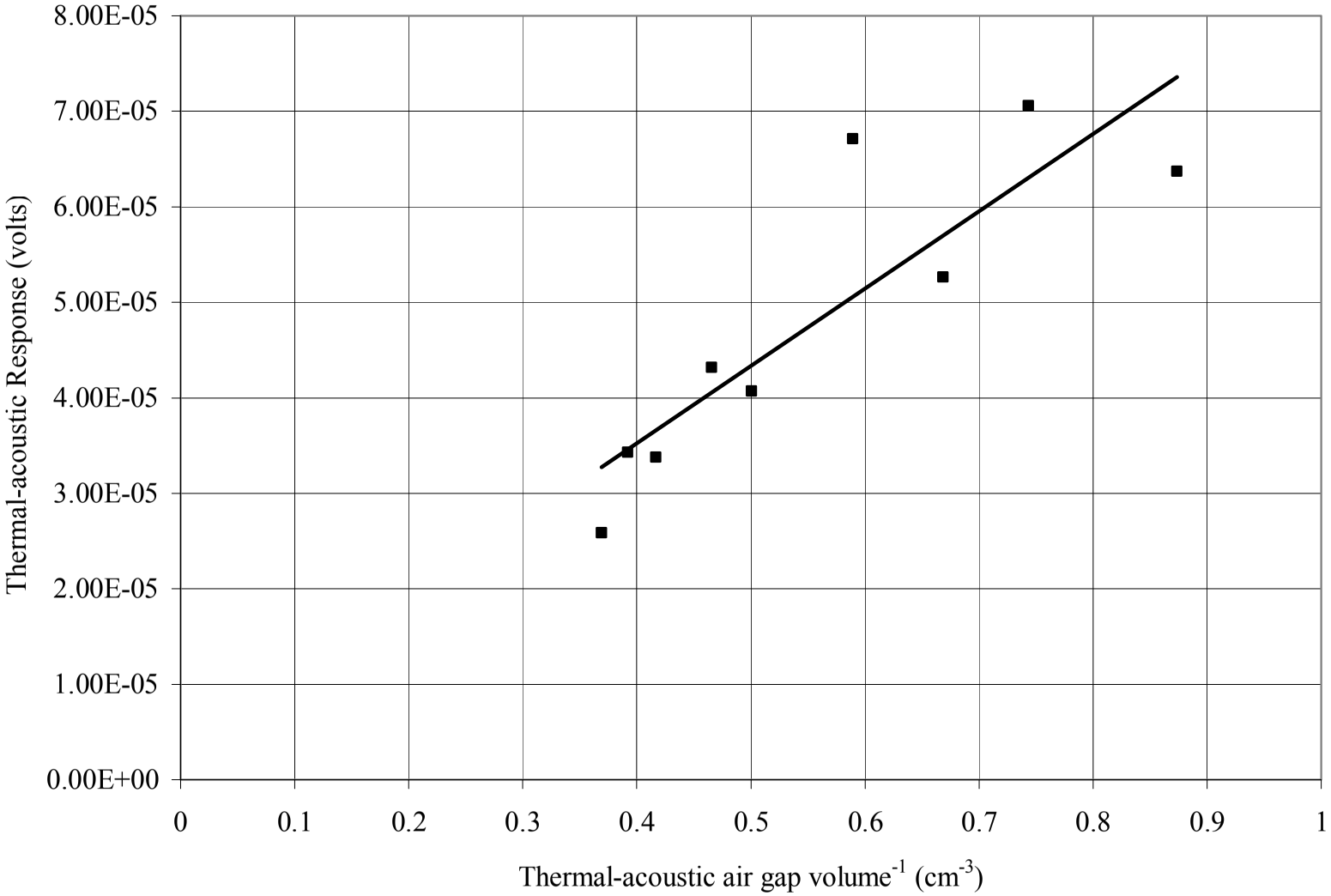

Figure 11. Thermal-acoustic response versus the inverse of the thermal-acoustic air gap volume. $R^2 = 0.755$.

Variations in bulk densities can also be compensated for in a similar manner, although the thermal-acoustic response is proportional to the inverse of the square-root of the powder density.

The third objective was to explore whether inorganic mineral matter in the fly ash may contribute to the overall thermal-acoustic response of the fly ash. Anecdotal evidence suggested that the thermal-acoustic response did not accurately correspond to carbon content of fly ashes for carbon content less than 2.0%, as determined by loss-on-ignition (LOI) analysis. Generally, very low carbon content flyashes produced much larger thermal-acoustic responses than expected. Chemical analyses were performed on several fly ashes of different carbon contents to determine their mineral content. The results are presented in **Table 5a** and **5b** of **Appendix C**. To determine if any of the major mineral constituents may contribute to the overall thermal-acoustic signal, pure samples of selected minerals were analyzed in the off-line monitor, and the results are presented in **Table 4**.

Table 4 shows that several minerals that are typically found in fly ash produce small but measureable thermal-acoustic responses. Of particular interest is silicon dioxide (SiO_2) because it represents a significant fraction of the mineral matter in fly ash (>40%), and iron (III) oxide (Fe_2O_3) because of its relatively strong thermal-acoustic response. Based on the data presented in **Tables 4**, as well as **Tables 5**, and **5a** of **Appendix C**, it was hypothesized that the overall thermal-acoustic response of fly ash could be expressed as the thermal-acoustic response of the individual components of the fly ash:

Table 4. Mineral matter present in fly ash known to produce a thermal-acoustic response.

Mineral	Thermal-acoustic response (air gap and density compensated) (volts)
CaO	1.26×10^{-5}
SiO_2	5.07×10^{-5}
Al_2O_3	1.89×10^{-5}
MgO	4.27×10^{-5}
Fe_2O_3	1.45×10^{-4}

$$PA_{response} = x_c \cdot PA_{unburned\ carbon} + (1 - x_c) \cdot PA_{\min eral\ matter} \quad \textbf{(14)}$$

with

$$PA_{\min eral\ matter} = \sum_i x_{m,i} \cdot PA_{m,i} \quad \textbf{(15)}$$

where $PA_{response}$ is the measured thermal-acoustic response of the fly ash (density-compensated), $PA_{unburned\ carbon}$ is the thermal-acoustic response due to the unburned carbon in fly ash, $PA_{mineral\ matter}$ is the thermal-acoustic response due to mineral matter in the fly ash, x_c is the mass fraction of carbon in the fly ash, $x_{m,i}$ is the mass fraction of species *i* that makes up the mineral matter of the fly ash (carbon-free basis), and $PA_{m,i}$ is the thermal-acoustic response of pure species *i* (density-compensated). From the two previous equations it is possible to determine the percentage of the measured thermal-acoustic signal that is due to mineral matter rather than unburned carbon.

Figure 12 shows the thermal-acoustic response of several different fly ashes, and also the calculated percentage of the thermal-acoustic response that is due to the presence of mineral matter. The plot demonstrates how the thermal-acoustic response can over-estimate the carbon content of fly ashes, especially those of low carbon content, because of the presence of microwave-absorbing inorganic mineral matter. Thus, the background signal from mineral matter must be accounted for in fitting the experimental data to a linear correlation if low carbon concentrations are to be accurately predicted. This was done in **Figure 12** by excluding the three fly ashes with carbon contents less than 2% from the regression analysis and assuming a constant background signal for the fly ashes with carbon content below this threshold. In this manner, a regression line with $R^2 = 0.958$ was obtained.

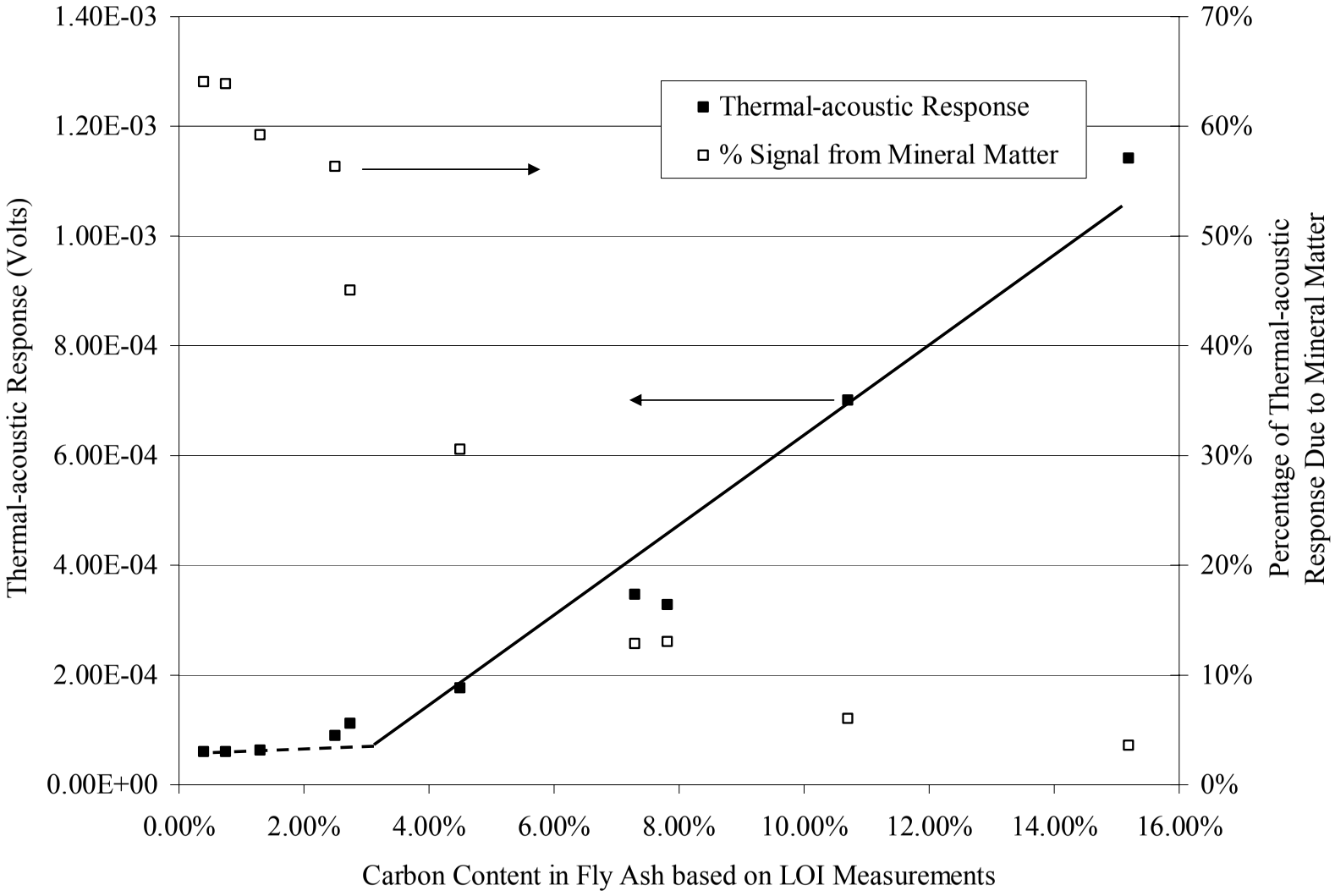

Figure 12. Influence of mineral matter in fly ash on the thermal-acoustic response. R^2=0.958.

The fourth objective was to demonstrate that the off-line fly ash monitor can predict the unburned carbon content in fly ash. **Figure 13** shows the thermal-acoustic response of 31 different fly ashes, listed in **Table 6** of **Appendix C**. The data demonstrate a linear relationship between the thermal-acoustic signal and the carbon content of the fly ash with an $R^2 = 0.778$. However, there were four samples that produced anomalous readings. Upon visual inspection, these fly ashes appeared to be mixtures of two types of different-colored particles, the majority of which were dull gray while the rest were a lighter-density black powder; their chemical composition and the reasons for their anomalous response to microwaves are not known. Although they are included in **Figure 13**, they were excluded in the regression analysis of the rest of the data. The data appears to be highly correlated below 12.0% carbon content, which includes most typical coal fly ashes, and less well correlated at higher carbon concentrations.

In the earlier stages of completing this objective, it was determined that there were some stability issues with the power level of the microwaves, so slight adjustments were made to the control-loop circuitry, resulting in a slightly lower, but more stable, power level of the microwaves. This would explain why the data in **Figure 13** appears not to correspond to data in **Figure 12**. However, the data for **Figure 13** was collected in less than one week's time, so if there were any instabilities present, they would be quite small and nearly undetectable.

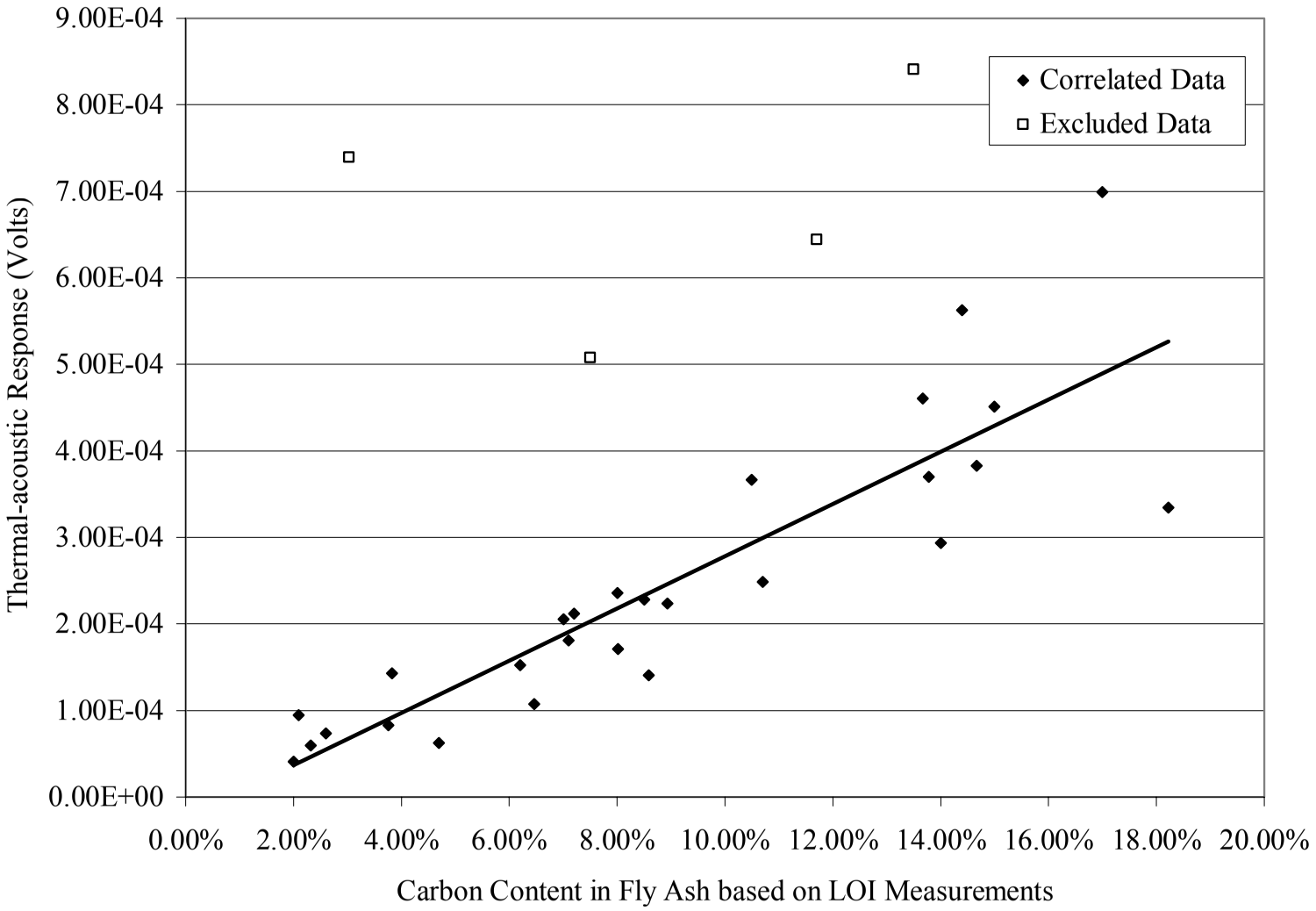

Figure 13. Thermal-acoustic response of fly ash in the off-line monitor. R^2=0.778.

Phase 2 – Broadband Off-line Thermal-acoustic Spectrometer

A thermal-acoustic microwave spectrum of a sample is a compilation of individual measurements performed at discrete microwave frequencies. The off-line fly ash monitor did not measure the thermal-acoustic response of a sample for a range of microwave frequencies simultaneously, but rather a single measurement was performed at a single microwave frequency, and then the microwave frequency was changed, and the measurement repeated.

Experiments were performed on three different types of samples: six different fly ashes ranging in carbon content from 0.4% – 4.5%, eight different coals of various rank and volatiles content, and six different minerals thought to be present in fly ash and/or coal. The spectral range of all broadband experiments was 500 – 1000 MHz with a resolution of 50 MHz. Each measurement took two minutes, and approximately 90 data points were collected and averaged. The lock-in amplifier conditions were: band-pass filter on, line filter on, line X2 filter on, and 1 second pre-time constant was used.

Figure 14 is a plot of the thermal-acoustic microwave spectra of the six fly ash samples investigated. The most dramatic difference between the individual spectra is the baseline shift of the spectra. The fly ash with the highest carbon content produced the greatest thermal-acoustic response, an expected result based on the results of single-frequency off-line experiments. The magnitude of the thermal-acoustic response for an individual spectrum also increases with increased microwave frequency, i.e. with increased energy intensity. To emphasize the subtle differences between spectra, they were normalized by forcing the minimum of each spectrum to a value of zero, and forcing the maximum of each spectrum to a value of one, as shown in **Figure 15**. This reduces the effect of a shifted spectral baseline, and emphasizes curvature variations of the spectra.

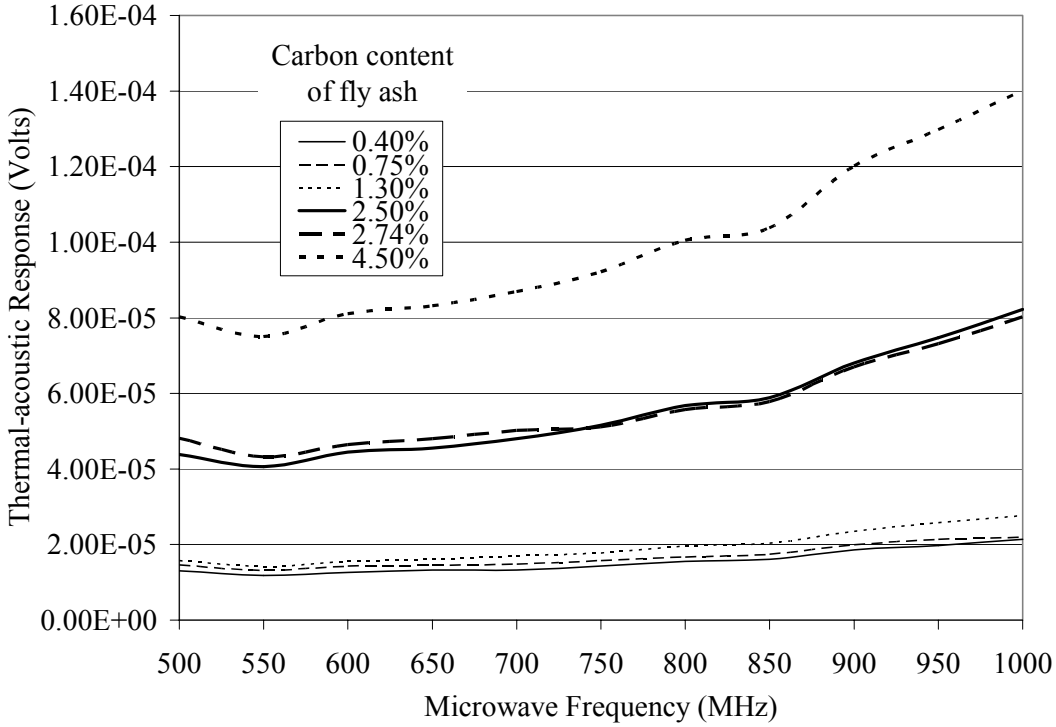

Figure 14. Thermal-acoustic microwave spectra of selected fly ashes.

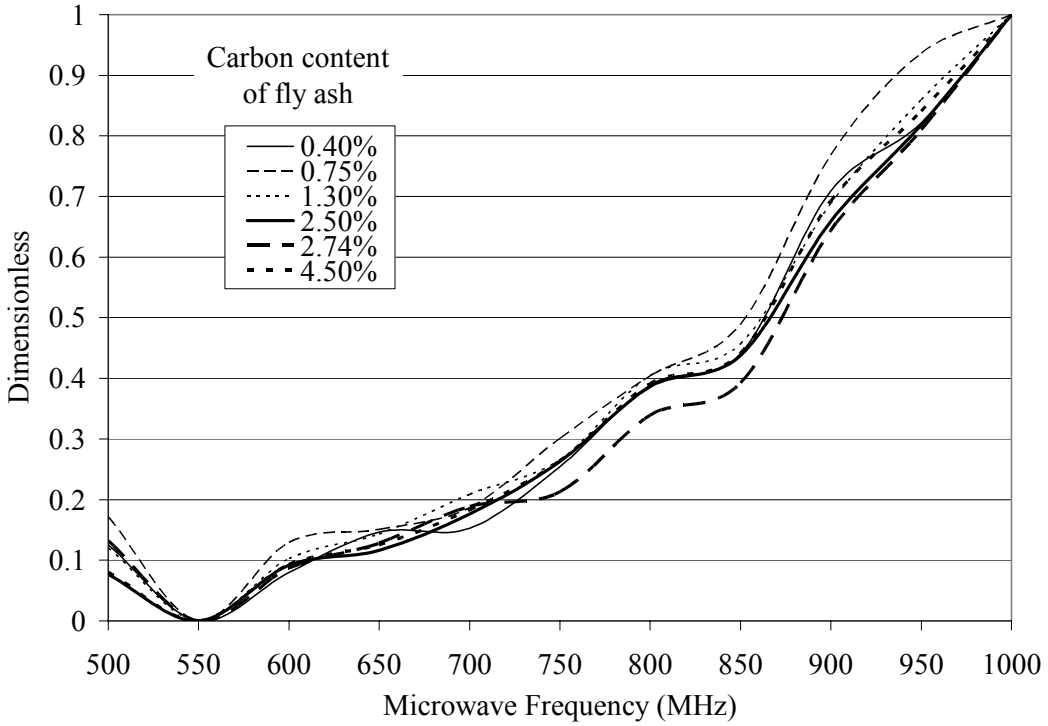

Figure 15. Normalized thermal-acoustic microwave spectra of selected fly ashes.

All six normalized fly ash spectra demonstrate some similar curvature features, such as the minimum occurs for each at 550 MHz and the presence of a shoulder at 800 MHz. But there are also differences apparent in the normalized spectra, particularly in the regions of 600 – 750 MHz and 850 – 950 MHz. It is unclear at this time what may cause these variations, but are most likely due to variations in mineral content.

Figures 16 and **17** are microwave thermal-acoustic spectra of eight different coals of various ranks. **Figure 16** is the unprocessed microwave spectra of the coals, and **Figure 17** is the normalized spectra of these coals, normalized in the same manner described previously. **Table 7** of **Appendix C** identifies the coals by rank. The normalized coal spectra are similar to the normalized fly ash spectra, where the local minimum occurs at 550 MHz, and a shoulder appears at 800 MHz. However, there are some differences between the coal spectra, most notably the absence of the shoulder at 800 MHz for DECS-27 and DECS-30, and the presence of a valley at 700 MHz for DECS-26, but additional investigation would be required to explore the nature of these variations.

Figures 18 and **19** are microwave thermal-acoustic spectra of selected pure minerals commonly found in fly ash, where **Figure 18** is of the unprocessed microwave spectra of the minerals, and **Figure 19** is of the normalized spectra. The normalized spectra demonstrate that the minerals exhibit a wide variety of interesting spectroscopic features. Both iron oxides, Fe_2O_3 and Fe_3O_4, are relatively featureless, except for a slight shoulder at 600 MHz, and a local minimum at 550 MHz. Iron sulfide, FeS, absorbs microwaves similar to the iron oxides at low microwave frequencies, but absorbs comparatively stronger at higher microwave frequencies, approximately in the range of 800 – 1000 MHz. Silicon dioxide, SiO_2**,** demonstrates the beginning development of a shoulder near 800 MHz, but further analysis should be conducted to

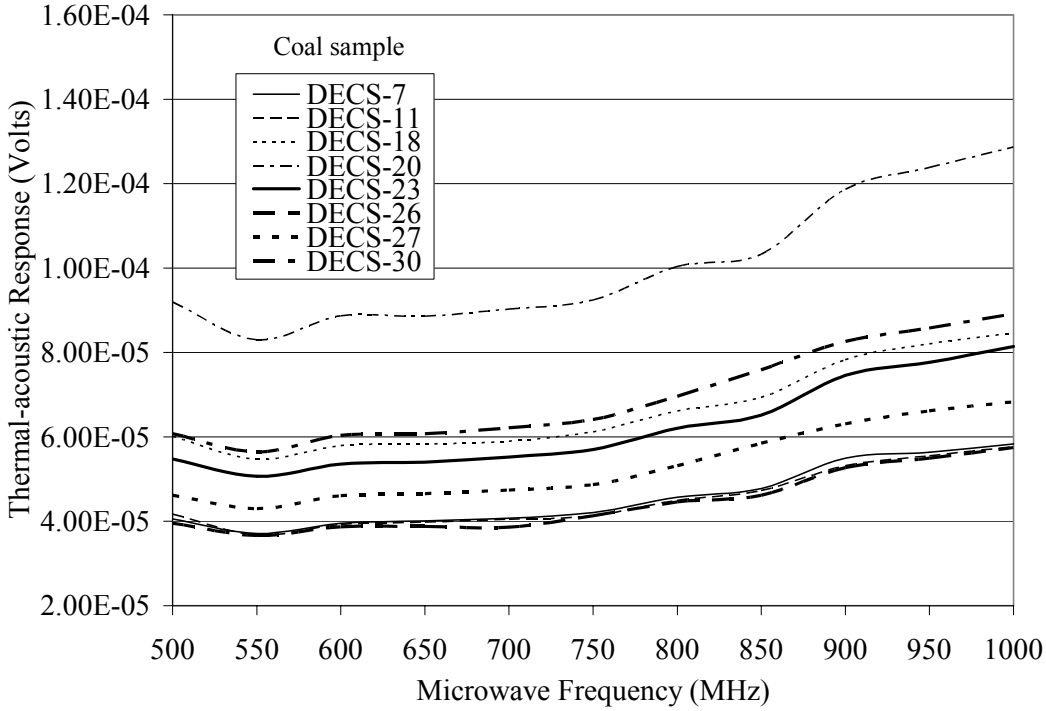

Figure 16. Thermal-acoustic microwave spectra of selected coal samples.

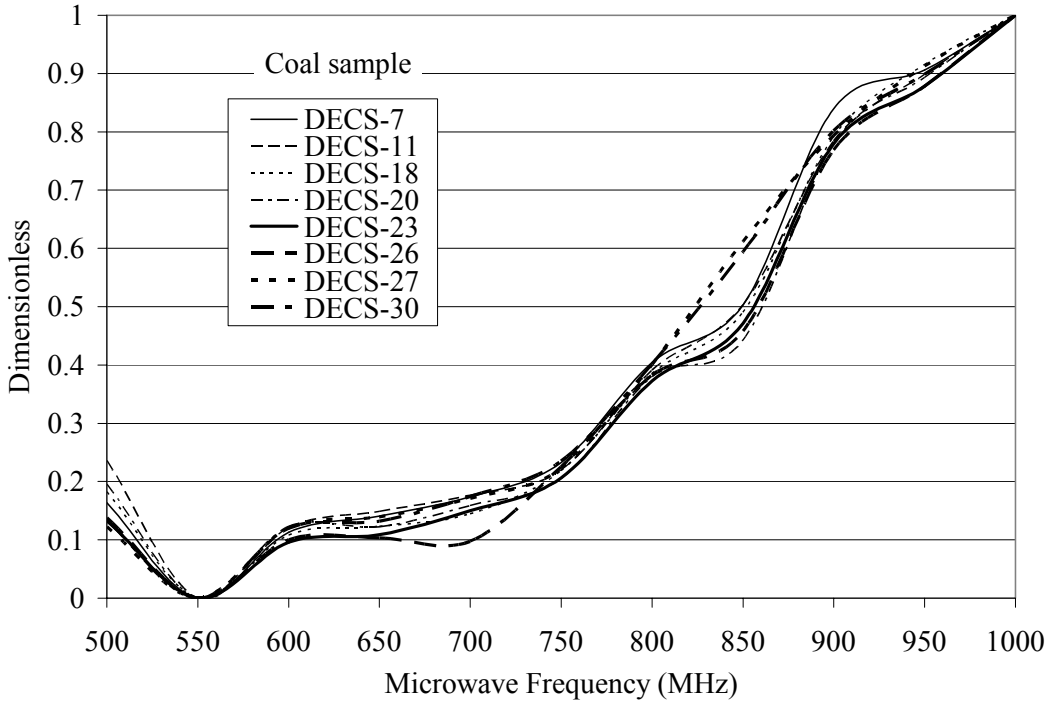

Figure 17. Normalized thermal-acoustic microwave spectra of selected coal samples.

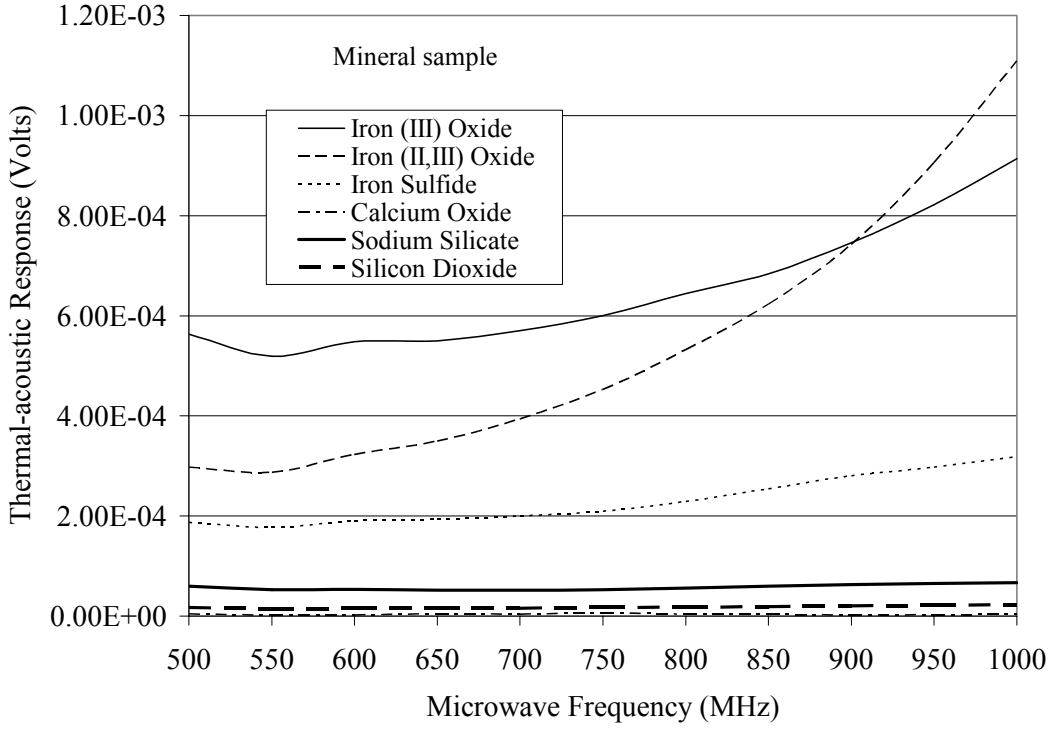

Figure 18. Thermal-acoustic microwave spectra of selected minerals.

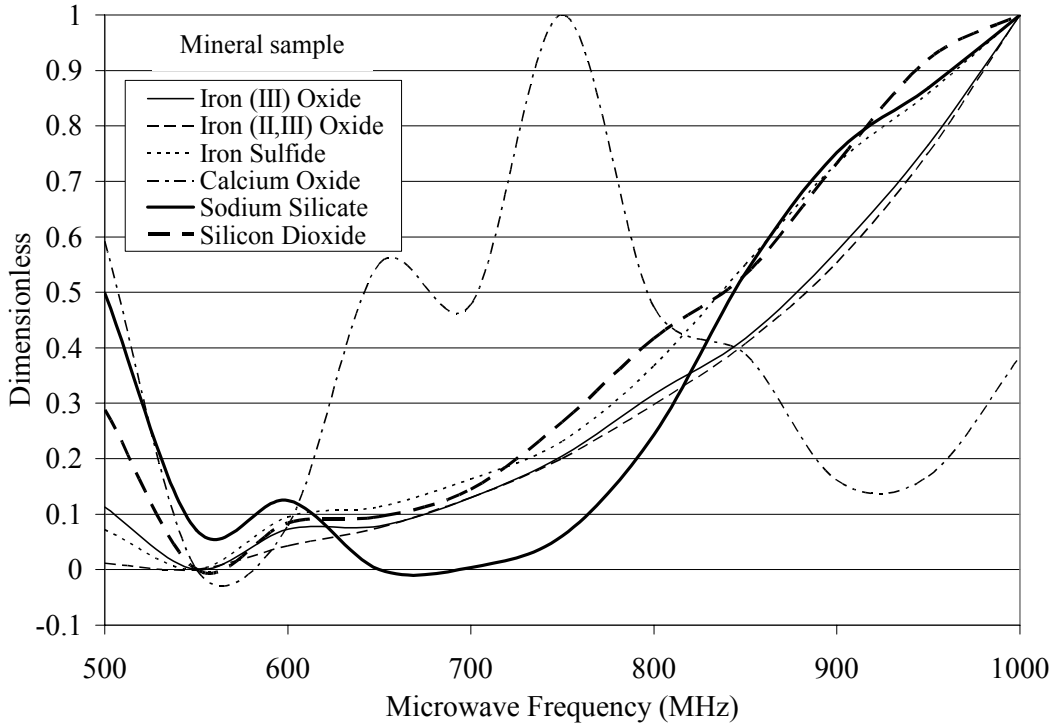

Figure 19. Normalized thermal-acoustic microwave spectra of selected minerals. Negative values are an artificial artifact of the smoothing function used to graphically display the spectra.

confirm that feature. The microwave spectra of sodium silicate, Na_2SiO_3, and calcium oxide, CaO, however, are very different from the other mineral spectra, the coal spectra, and the fly ash spectra. The minimum for Na_2SiO_3 occurs not at 550 MHz, but near 650 MHz, where there is a broad basin between 650 – 750 MHz. Calcium oxide on the other hand, is the only species for which the maximum does not occur at 1000 MHz, but rather at 750 MHz, with another, smaller peak occurring at 650 MHz. Some of the spectra appear to have negative values at certain microwave frequencies, but these negative values are simply an artifact of the smoothing function used by Microsoft Excel in generating these plots.

Figures 14 – 19 demonstrate that there are spectral differences among the different fly ashes, coal, and inorganic minerals, but significant improvements of the methodology for collecting and generating these spectra need to be made. Two possible improvements include increasing the resolution of the spectra and establishing a baseline spectrum.

Subtle differences in the normalized spectra may become more pronounced with increased spectral resolution, but the present method of manually interrogating the samples at different frequencies precludes the generation of high-resolution spectrum with the current equipment. A computer-controlled, variable-frequency microwave source that could sweep through the desired bandwidth range automatically would make the spectrometer much more powerful as an analytical tool.

Identifying a baseline spectrum and then comparing a sample spectrum with the baseline spectrum would not only enhance spectral features by mathematically eliminating spectral features that are common to all samples (features that are due to the physical equipment), but would also establish a standard that could be used to calibrate other off-line microwave-excited thermal-acoustic spectrometers.

Phase 3 – Single-Frequency On-line Fly Ash Monitor

On-line thermal-acoustic fly ash experiments

Microwave-excited thermal-acoustic experiments were conducted on six fly ashes in the on-line fly ash monitor. The measurements were made under non-flowing conditions. The settings for the lock-in amplifier where: band-pass filter on; line filter on; line X2 filter on; and a 10 second pre-time constant was used. **Figure 20** shows the thermal-acoustic responses of fly ashes for different unburned carbon contents. Initial observation indicated a poor linear correlation with an $R^2 = 0.359$. However, if the data is adjusted to compensate for differences in bulk density for the various fly ashes, then the correlation improves dramatically to $R^2 = 0.830$. Based on the data presented in **Figure 20**, an on-line microwave-excited thermal-acoustic fly ash monitor can be used to quantify the unburned carbon content in fly ash when operated under quasi-steady state conditions, assuming the bulk density of the fly ash is known.

On-line thermal-elastic fly ash experiments

On-line thermal-elastic fly ash experiments were conducted over a seven-week period from July 13, 2004 – August 31, 2004. All data shown in the following figures are averages of up to five trials conducted during this time period.

Figure 21 is of the microwave-induced thermal-elastic response of the fly ash in the on-line monitor under flowing and non-flowing conditions, and compares these results to baseline thermal-elastic responses (no microwaves present). Only data from the test accelerometer was recorded (the differential op-amp circuitry was by-passed). The data indicate that while the fly ash does exhibit a thermal-elastic effect due to the microwaves, there was no apparent correlation between the intensity of the thermal-elastic response and the carbon content of the fly ash.

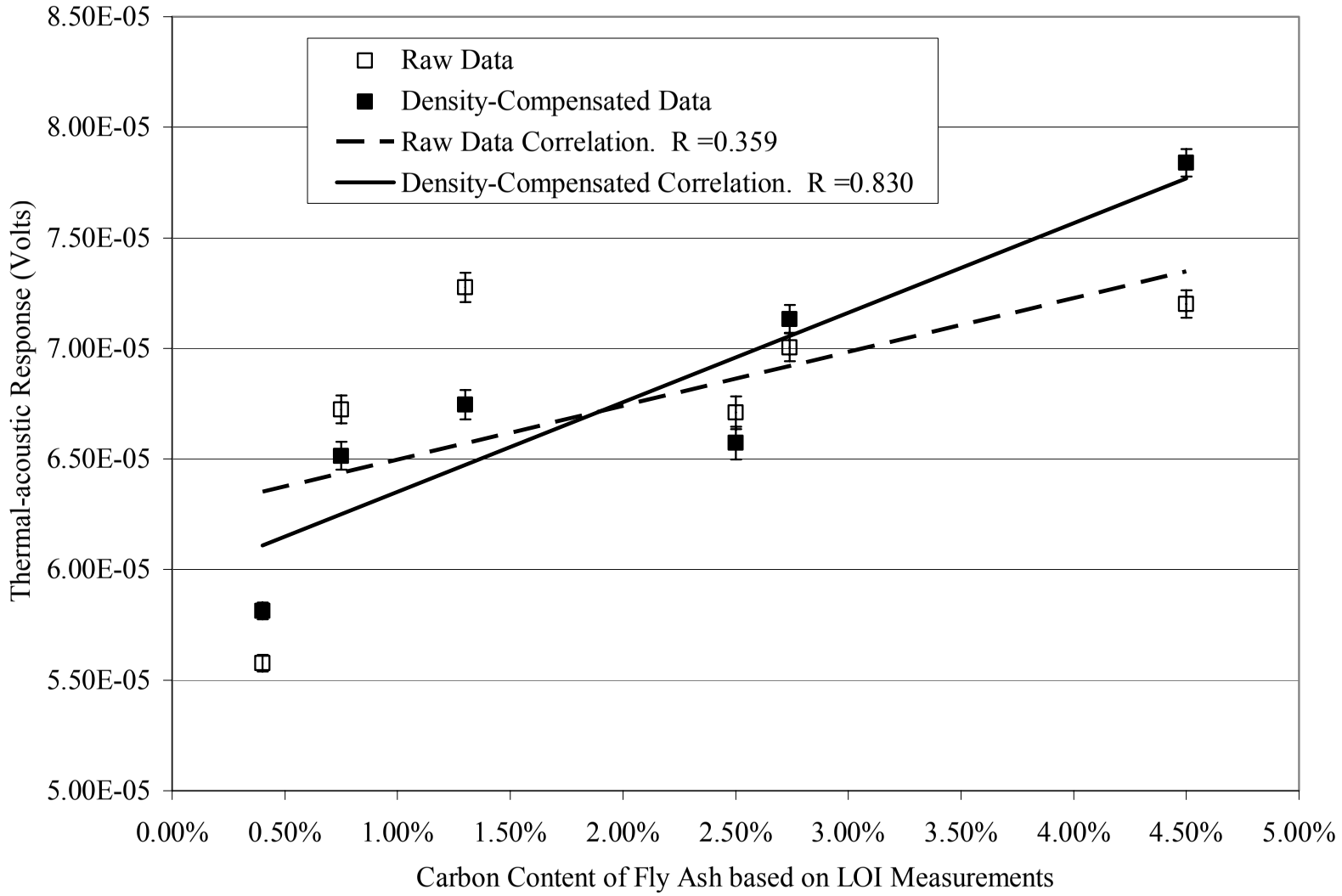

Figure 20. Thermal-acoustic response of fly ash in the on-line fly ash monitor. Non-flowing condition. Error bars are 95% confidence intervals.

Figure 22 is of the microwave-induced thermal-elastic response of the fly ash in the on-line monitor under flowing and non-flowing conditions when both accelerometers ("test" and "control" are operational; these results are also compared to baseline thermal-elastic responses (no microwaves present). The signal outputs from both accelerometers were fed into the differential op-amp circuitry to actively cancel out background noise and vibrations due to the flowing fly ash particles. It should be noted that the op-amp provides an average overall signal gain of approximately 1.9, which would explain the greater signal strength as compared to the data shown in **Figure 21**. There was still no apparent correlation between carbon content and the thermal-elastic response induced by the microwaves and detected by the accelerometers.

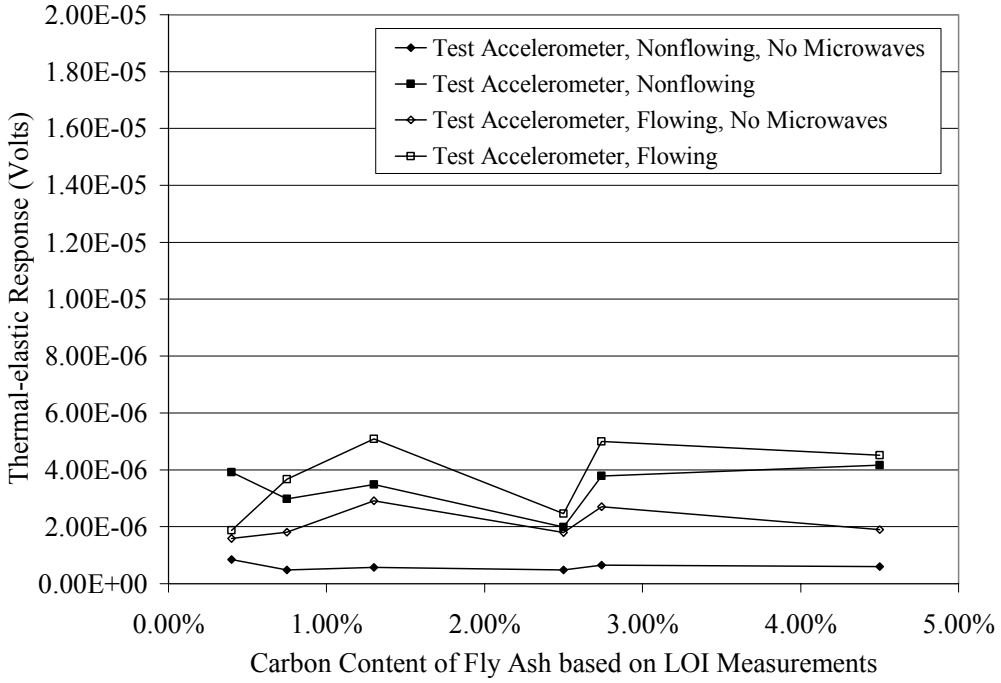

Figure 21. Thermal-elastic response of fly ash in the on-line monitor operated under non-flowing and flowing conditions. Response was from the test (or bottom) accelerometer only.

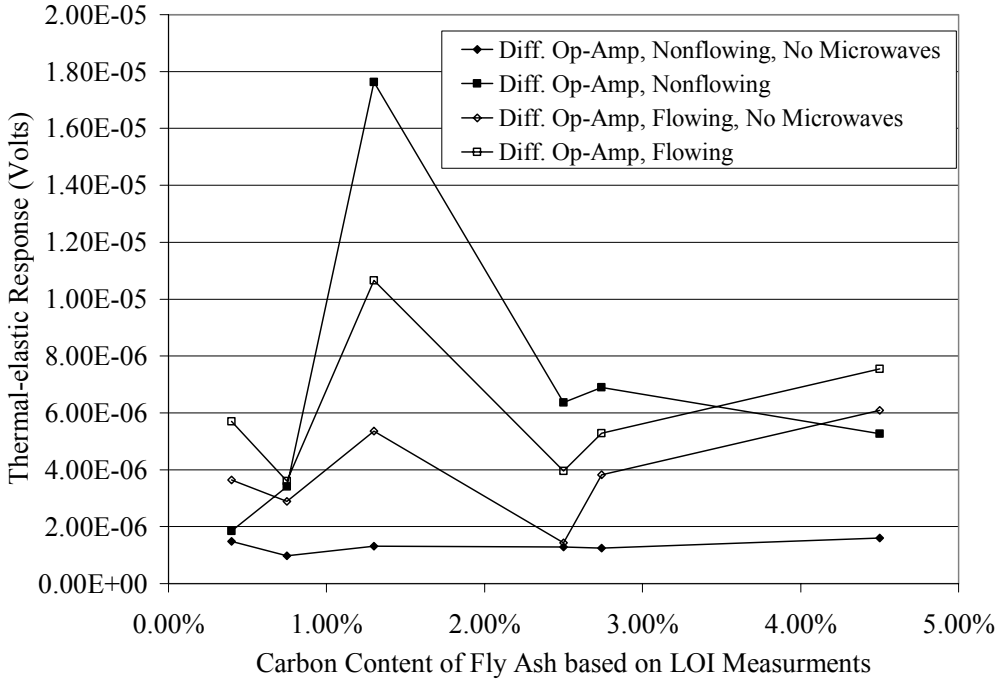

Figure 22. Thermal-elastic response of fly ash in the on-line monitor operated under non-flowing and flowing conditions. Both accelerometers were in operation, and the signal shown here is the output voltage from the instrumentation-quality differential op-amp with an average gain of 1.9.

CONCLUSION

This research was divided into three phases. The first phase focused on single-frequency, off-line experiments that explored the effect of sample handling and instrument parameters on the thermal-acoustic signal. The second phase focused on generating microwave spectra of various powders to determine if this information was useful for analyzing sample composition. The third phase translated the single-frequency, off-line instrument into an on-line version for analyzing unburned carbon content of fly ash. Both thermal-acoustic and thermal-elastic effects, excited by microwaves, were employed in this third manifestation of the instrument.

The first phase of research demonstrated that modulating 1 GHz microwaves at 20 Hz was ideal for interrogating samples. Compressing the samples resulted in stronger signals than uncompressed samples. The thermal-acoustic response was proportional to the inverse of the thermal-acoustic volume, agreeing with theory. Variations in sample moisture content were minimal so that the effect on the thermal-acoustic response was negligible. Variations in ambient humidity and temperature also produced negligible effects on the thermal-acoustic response. The research also demonstrated that the presence of silicon dioxide and iron (III) oxide generated a background thermal-acoustic signal, which can be a problem for fly ashes with carbon content less than 2%. Nevertheless, in the range of 2% – 18% carbon content, the off-line thermal-acoustic instrument was able to correlate thermal-acoustic signal to carbon content of a random collection of fly ashes with a correlation constant of $R^2 = 0.778$.

In the second phase of research, microwave spectra of fly ash, coal, and pure minerals were generated using the thermal-acoustic effect. Spectral differences could be distinguished among these materials, but improved spectral resolution is required before the technique is applied for either qualitative or quantitative analysis of mineral content. The use of a broadband

microwave source, rather than the tunable, single-frequency microwave source employed in this study, would greatly enhance this opportunity for spectral analysis.

The third phase of the research demonstrated the thermal-acoustic method was able to predict the carbon content of the fly ash, with a linear correlation constant of $R^2 = 0.830$ for the limited collection of fly ashes employed in this analysis. The use of a preamplifier with the microphone might have improved the performance of this device. On the other hand, the thermal-elastic method was unsuccessful at predicting the carbon content of fly ash. Improvements might include developing a better way to secure the accelerometer to the aluminum diaphragm, and modifying the design of the on-line monitor so as to precisely control the alignment of the diaphragm, as well as the applied tension of the diaphragm.

ACKNOWLEDGEMENTS

The authors would like to thank King-Sang Chan, Maohong Fan, Nick Lucas, Tyrone Moore, and Andy Suby for their assistance with this research, and Susan Maley of NETL for her advice and direction for this research. The U.S. Department of Energy provided the funding through award #DE-FC22-01NT41220.

BIBLIOGRAPHY

1. Rosencwaig, A. (1980) “Thermal-acoustics and Thermal-acoustic Spectroscopy,” Wiley, New York.
2. Rosencwaig, A. and Gersho, A. (1976) “Theory of the thermal-acoustic effect with solids.” *J. Appl. Phys*., 47(1), 64.
3. Rosencwaig, A. (1977) “Solid State Thermal-acoustic Spectroscopy.” In *Optoacoustic Spectrosocopy and Detection*, Pao, Y. H., ed. Academic Press, New York.
4. McClelland, J. F. (1983) “Thermal-acoustic Spectroscopy.” *Anal. Chem*., 55(1), 89a.
5. McClelland, J. F. and Kniseley, R. N. (1976) “Thermal-acoustic spectroscopy with condensed samples.” *Appl. Opt*., 15(11), 2658.
6. McDonald, F. A. and Wetsel, G. C. Jr. (1978) “Generalized theory of the thermal-acoustic effect.” *J. Appl. Phys*., 49(4), 2313.
7. McClelland, J. F., Jones, R. W., Luo, S., and Seaverson, L. M. (1993) “A Practical Guide to FT-IR Thermal-acoustic Spectroscopy.” In *Practical Sampling Techniques for Infrared Analysis*, Coleman, P. B., ed. CRC Press, Boca Raton, Florida.
8. Waller, D. J. and R. C. Brown (1996) "Thermal-acoustic response of unburned carbon in fly ash to infrared radiation," Fuel 75, 1568-1574.
9. Gordy, W. and Cook, R. L. (1984) Microwave Molecular Spectra, John Wiley & Sons, New York.
10. Faxvog, F. R. and Roessler, D. M. (1979) Appl. Opt. 17, 2612.
11. Jones, A. R. (1979) “Scattering of electromagnetic radiation in particulate laden fluids,” Progress in Energy and Combustion Science, 5, 73-96.
12. Jackson, J. D. (1975) Classical Electrodynamics, 2nd Edition, Wiley, NY.

APPENDIX A – MATHCAD PROGRAM USED FOR DETERMINING THE ACCELEROMETER RESPONSE FOR A THERMAL-ELASTIC WAVE

Pre-constants

$a := 0..5 \qquad b := 0..5$ Vector indices

Operating parameters and fly ash monitor physical characteristics

$\omega := 1000\,Hz$ Modulation frequency

$Power_0 := 7 \cdot W$ Incident power

$Temp := 293.55\,K$ Ambient Temperature

$u := 1.0625\,in$ Thickness of fly ash in sample chamber

$Area := 1.625\,in \cdot 2.625\,in \qquad Area = 4.266\,in^2$ Area of diaphragm

$t_d := 0.002\,in$ Thicknesses of diaphragm

$\rho_d := 2702 \cdot \frac{kg}{m^3}$ Density of aluminum diaphragm

$mass_d := \rho_d \cdot t_d \cdot Area \qquad mass_d = 0.378\,gm$ Mass of diaphragm

$mass_{acc} := 7.5 \cdot gm$ Mass of accelerometer

$$x_c := \begin{pmatrix} 0.004 \\ 0.0075 \\ 0.013 \\ 0.025 \\ 0.0274 \\ 0.045 \end{pmatrix}$$ Mass fraction of carbon in fly ash from LOI analysis

$$\rho := \begin{pmatrix} 1.30 \\ 1.40 \\ 1.46 \\ 1.39 \\ 1.33 \\ 1.25 \end{pmatrix} \cdot \frac{gm}{cm^3}$$ Measured bulk density of fly ash samples

$Cp := 1.3187 \cdot \frac{joule}{gm \cdot K}$ Heat capacity of fly ash

$B := 5 \cdot 10^7 \cdot \frac{dyne}{cm^2}$ Bulk modulus of fly ash

$\alpha_{exp} := 9 \cdot 10^{-6} \cdot K^{-1}$ Coefficient of thermal expansion for fly ash

$\beta_0 := 0.201 \cdot m^{-1}$ Optical absorption coefficient for 1.0% CC

$\beta := \frac{\beta_0}{0.01} \cdot x_c$ $\beta = \begin{pmatrix} 0.08 \\ 0.151 \\ 0.261 \\ 0.503 \\ 0.551 \\ 0.905 \end{pmatrix} m^{-1}$ Assumes Beta is proportional to CC

$Power\_abs := Power_0 \cdot \left(1 - e^{-u \cdot \beta}\right)$ $Power\_abs = \begin{pmatrix} 0.015 \\ 0.028 \\ 0.049 \\ 0.094 \\ 0.103 \\ 0.169 \end{pmatrix} W$ Absorbed Power

$\theta_a := \frac{Power\_abs_a}{\omega \cdot \rho_a \cdot Cp \cdot Area \cdot u}$ $\theta = \begin{pmatrix} 1.192 \times 10^{-7} \\ 2.073 \times 10^{-7} \\ 3.44 \times 10^{-7} \\ 6.926 \times 10^{-7} \\ 7.928 \times 10^{-7} \\ 1.379 \times 10^{-6} \end{pmatrix} K$ Temperature rise in sample

$Pressure := B \cdot \alpha_{exp} \cdot \theta$ $Pressure = \begin{pmatrix} 5.362 \times 10^{-6} \\ 9.327 \times 10^{-6} \\ 1.548 \times 10^{-5} \\ 3.117 \times 10^{-5} \\ 3.568 \times 10^{-5} \\ 6.205 \times 10^{-5} \end{pmatrix} Pa$ Pressure from microwaves

$$acc := \frac{Pressure \cdot Area}{mass_{acc} + mass_{d}}$$

$$acc = \begin{pmatrix} 1.91 \times 10^{-7} \\ 3.323 \times 10^{-7} \\ 5.514 \times 10^{-7} \\ 1.11 \times 10^{-6} \\ 1.271 \times 10^{-6} \\ 2.21 \times 10^{-6} \end{pmatrix} g$$

Acceleration of diaphragm and accelerometer, assuming stiffness and dampening forces are negligible.

$$response := 1.171 \cdot \left[1 + \frac{75 \cdot 10^{-6}}{K} \cdot (Temp - 298 \cdot K) \right] \cdot \frac{V}{g} \cdot acc$$

Temperature-compensated signal response of accelerometer based on manufacturer's specifications

$$response = \begin{pmatrix} 2.236 \times 10^{-7} \\ 3.890 \times 10^{-7} \\ 6.455 \times 10^{-7} \\ 1.300 \times 10^{-6} \\ 1.488 \times 10^{-6} \\ 2.587 \times 10^{-6} \end{pmatrix} V$$

APPENDIX B – SCHEMATICS

Schematic 1. Main schematic of microwave generation and implementation for the fly ash monitor.

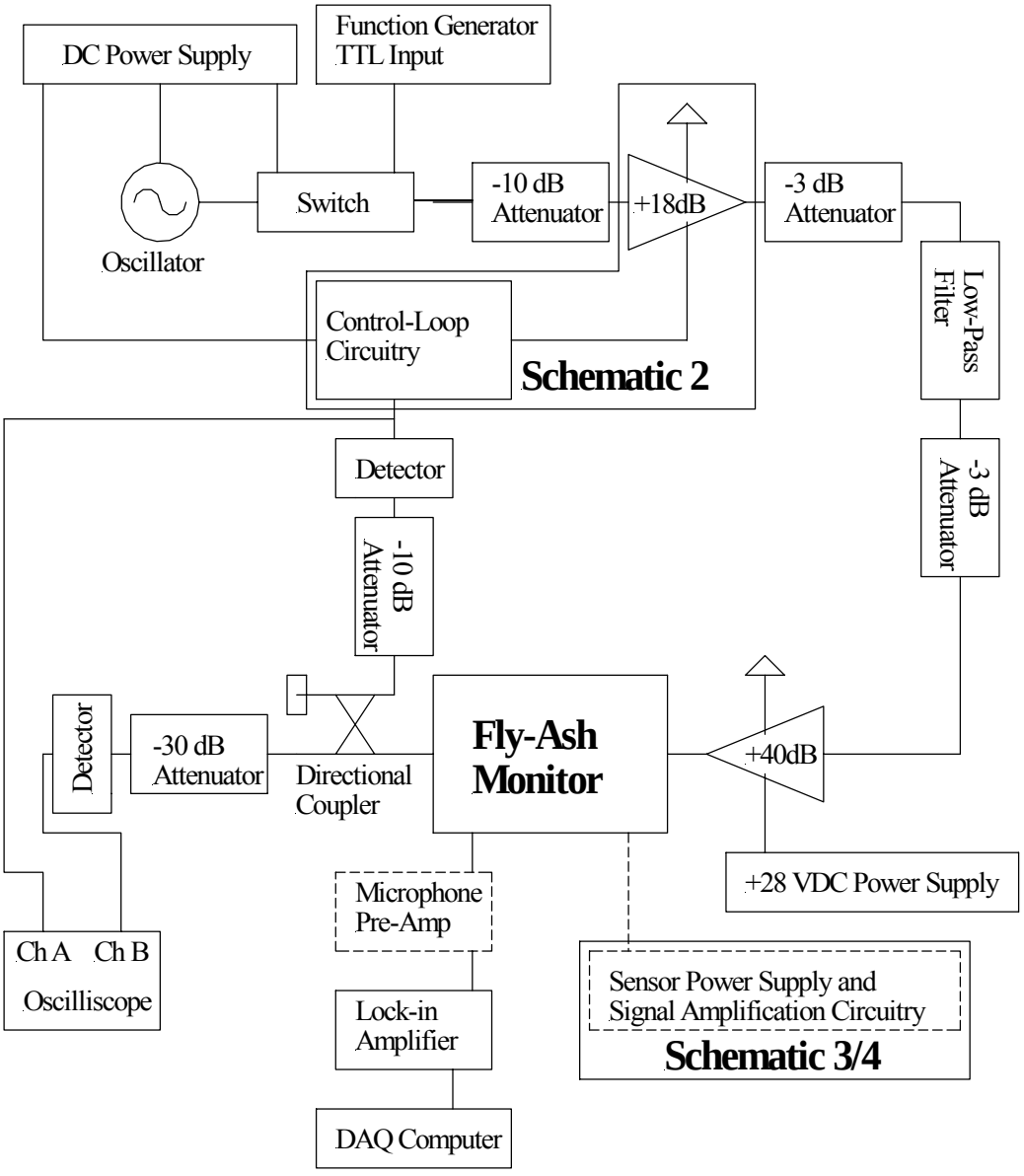

The microphone pre-amp is only used for off-line thermal-acoustic measurements, while the sensor power supply and signal amplification circuitry is only used for on-line thermal-acoustic (Schematic 3) or thermal-elastic (Schematic 4) measurements.

Schematic 2. Control-loop circuitry for maintaining proper microwave power levels.

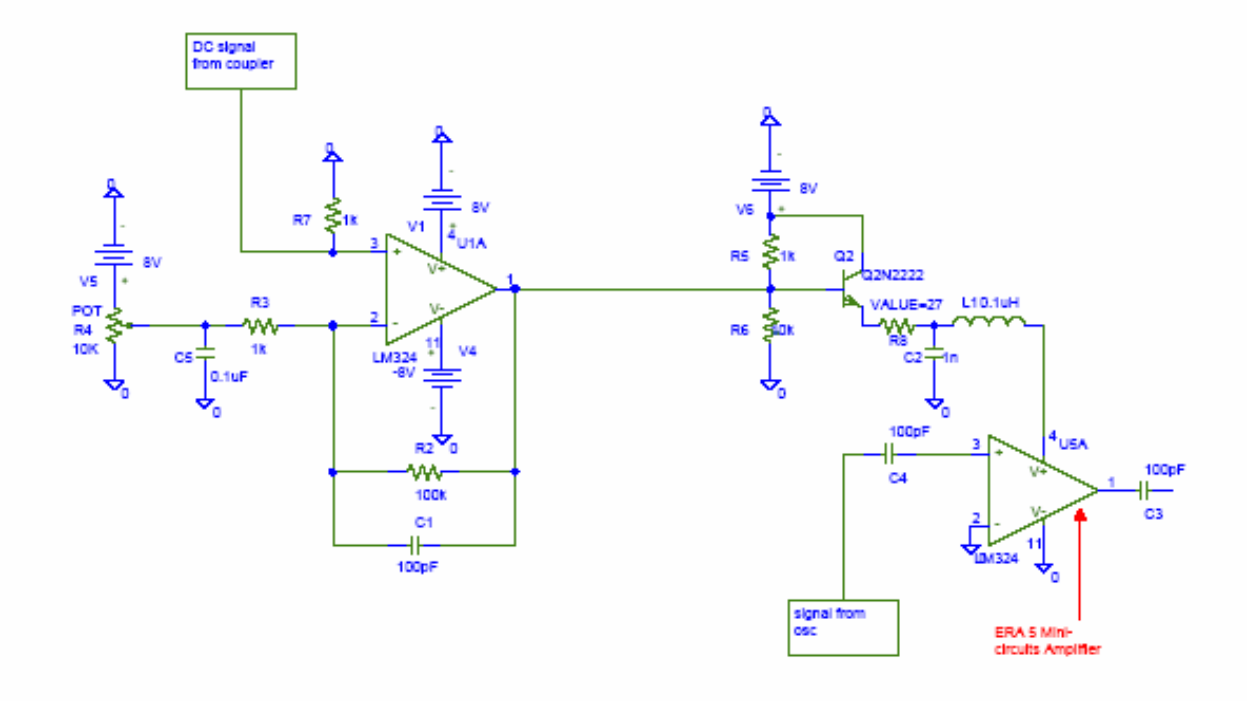

The DC signal from the directional coupler is combined with a DC voltage (adjusted with the R4 potentiometer) in the LM324 op-amp produces a DC output. This DC output then is used to control the gain of the ERA 5 Mini-Circuits Amplifier, which amplifies the microwave power level from the oscillator. Lead 1 from the ERA 5 amplifier is the output of the microwaves.

Schematic 3. Bias circuitry used by the microphone when conducting on-line thermal-acoustic measurements.

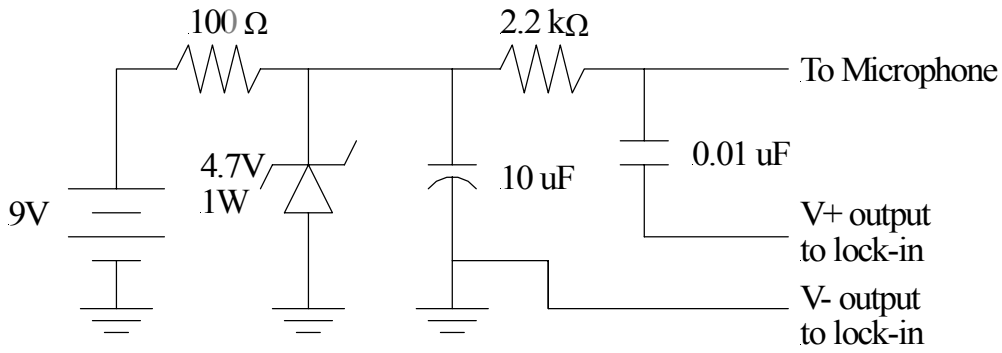

This biasing circuitry was used to power the microphone used for on-line thermal-acoustic measurements.

Schematic 4. Instrumentation-quality differential operational-amplifier designed for active noise control.

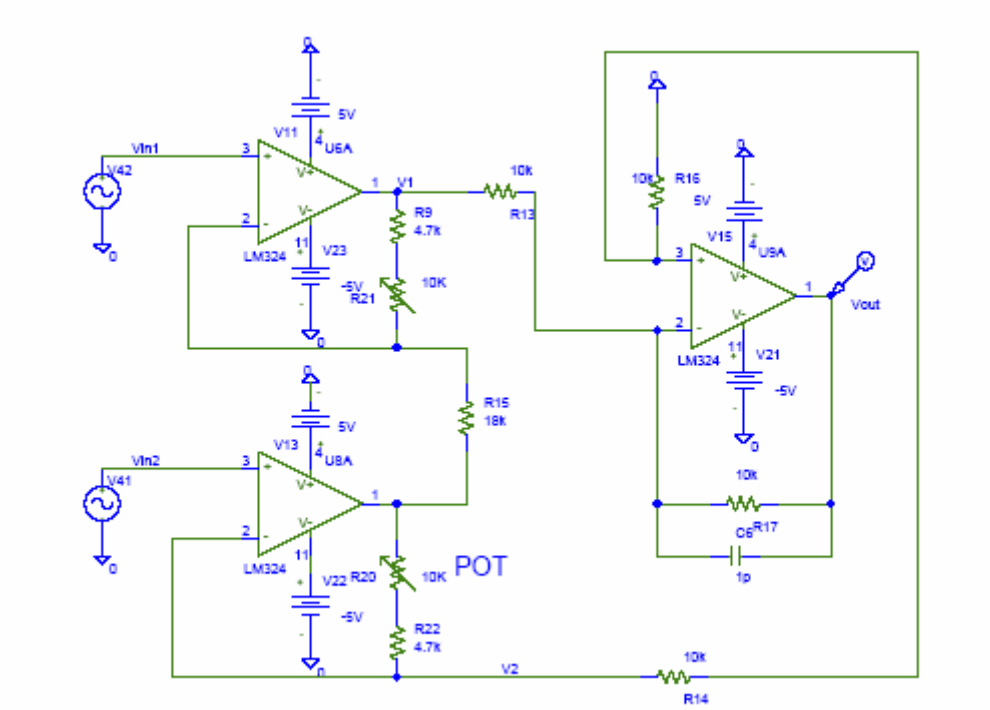

This circuitry provides active noise control when the two accelerometers were used in parallel for quantifying the microwave-induced thermal-elastic wave in the fly ash in the on-line fly ash monitor. The objective of the circuitry was to subtract out any vibrations that were common to both accelerometers (laboratory vibrations or acoustical noise or internal fluctuations due to the random nature of the flowing fly ash particles), thereby isolating vibrations caused only by the microwaves, which were contained solely within the test region of the fly ash monitor. Two potentiometers, R20 and R21, were adjusted to compensate for the fact that voltage responses of the two accelerometers were not identical, i.e. the top (or control) accelerometer (Vin2) produces 1.136 V g^{-1}, while the bottom (or test) accelerometer (Vin1) produces 1.171 V g^{-1}.

APPENDIX C – CHEMICAL ANALYSES AND SAMPLE LISTS

Tables 5a and **5b** list the fly ashes used to explore how the overall thermal-acoustic response might be influenced by mineral matter in fly ash. **Table 6** lists the fly ashes used to demonstrate how single-frequency off-line thermal-acoustic measurements are able to predict the unburned carbon content in fly ash. The four fly ashes in *italics* in **Table 6** were not included in the correlation analysis as shown in **Figure 13**. **Table 7** list the coal samples used for generating the microwave thermal-acoustic spectra as shown in **Figures 16** and **17**.

Table 5a. Fly ashes used in mineral matter analysis for Phase 1 research.

Sample Identification	Original Source	% Carbon Content Based on LOI
22368AT	Duquesne/Elrama 3B, PA	3.63%
22360AT	Duquesne/Elrama 3B, PA	7.30%
22342AT	Duquesne/Elrama 3B, PA	14.70%
22339AT	Duquesne/Elrama 3B, PA	10.70%
0.4%CC	Ames City Power Plant, IA	0.4%
0.75%CC	Hennepin Power Station, IL	0.75%
1.3%CC	Hennepin Power Station, IL	1.3%
2.5%CC	Hennepin Power Station, IL	2.5%
2.74%CC	Hennepin Power Station, IL	2.74%
4.5%CC	New York State Electric and Gas, NY	4.5%

Table 5b. Mineral content of fly ashes used in for Phase 1 research (carbon-free, % mass basis).

Sample	Al_2O_3	CaO	Fe_2O_3	MgO	P_2O_5	K_2O	SiO_2	Na_2O	SO_3	TiO_2
22368AT[1]	24.95	1.93	10.04	0.87	0.57	2.30	52.38	0.42	0.33	1.25
22360AT[1]	25.44	1.50	11.46	0.93	0.06	2.34	51.36	0.43	0.49	1.25
22342AT[1]	25.06	2.01	11.63	0.93	0.30	2.08	51.06	0.42	0.45	1.17
22339AT[1]	25.67	1.90	10.58	0.95	0.33	2.28	51.97	0.40	0.36	1.20
0.4%CC[2]	18.90	19.90	6.49	3.96	0.91	0.60	42.30	1.60	1.65	1.22
0.75%CC[2]	18.51	20.30	5.73	3.89	0.99	0.58	44.44	1.52	1.38	1.29
1.3%CC[2]	17.00	20.12	5.64	3.85	0.94	0.54	43.94	1.18	1.95	1.22
2.5%CC[2]	18.43	5.18	13.15	1.14	0.24	2.11	55.39	1.23	1.65	0.91
2.74%CC[2]	18.70	4.85	14.00	1.03	0.22	2.10	52.67	1.17	1.55	0.86
4.5%CC[2]	20.63	5.02	20.12	0.89	0.39	1.42	44.03	1.01	1.40	0.91

[1]Analysis conducted by Huffman Laboratories, Inc., Golden, CO.
[2]Analysis conducted by Minnesota Valley Testing Laboratories, Inc., Bismarck, ND.

Table 6. Fly ashes used to for thermal-acoustic measurements Phase 1 research.

Sample ID	Original Source	% Carbon Content based on LOI
21837AT	*Duquesne/Elrama3B, PA*	*11.70%*
21839AT	Duquesne/Elrama 4B, PA	6.20%
21846AT	Duquesne/Elrama 4B, PA	14.00%
21960AT	Duquesne/Elrama 3B, PA	18.22%
21964AT	Duquesne/Elrama 3B, PA	8.93%
21996AT	Duquesne/Elrama 3B, PA	14.67%
22001AT	Duquesne/Elrama 3B, PA	8.01%
22288AT	Duquesne/Elrama 2A, PA	13.67%
22336AT	Duquesne/Elrama 3B, PA	17.00%
22339AT	Duquesne/Elrama 3B, PA	10.70%
22343AT	Duquesne/Elrama 2A, PA	15.00%
22345AT	Duquesne/Elrama 3B, PA	14.40%
22348AT	*Duquesne/Elrama 3B, PA*	*13.50%*
22352AT	Duquesne/Elrama 3B, PA	7.10%
22356AT	Duquesne/Elrama 3B, PA	7.20%
22368AT	Duquesne/Elrama 3B, PA	7.01%
22372AT	Duquesne/Elrama 3B, PA	8.02%
22473AT	Duquesne/Elrama 2A, PA	10.50%
22499AT	Duquesne/Elrama 2A, PA	2.10%
22518AT	Duquesne/Elrama 3B, PA	2.60%
AM38	Hennepin Power Station, IL	4.70%
AM39	*Streeter/Cedar Falls Utilities, IA*	*3.03%*
AM40	Pell-Electric Department, IA	8.59%
AM41	Pell-Electric Department, IA	8.50%
AM46	Fort Drum Cogeneration, NY	2.00%
AM47	Fort Drum Cogeneration, NY	6.46%
AM56	Dunkirk Steam Station, NY	3.76%
AM57	*Dunkirk Steam Station, NY*	*7.50%*
AM70	UNC-CH Cogeneration Facility, NC	3.83%
AM71	UNC-CH Cogeneration Facility, NC	13.78%
AM72	J. H. Campbell Unit #2, MI	2.32%

Table 7. Coal samples provided by Pennsylvania State University Coal Sample Bank and Database used for Phase 2 research.

Sample ID	Original Source	Classification
DECS-7	Adaville #1 Seam, Lincoln Co., WY	High-volatile C bituminous
DECS-11	Beulah Seam, Mercer Co., ND	Lignite A
DECS-18	Kentucky #9 Seam, Union Co., KY	High-volatile B bituminous
DECS-20	Elkhorn #3 Seam, Floyd Co., KY	High-volatile A bituminous
DECS-23	Pittsburgh Seam, Washington Co., PA	High-volatile A bituminous
DECS-26	Wyodak Seam, Campbell Co., WY	Subbituminous B
DECS-27	Deadman Seam, Sweetwater Co., WY	Subbituminous A
DECS-30	Splash Dam Seam, Buchanan Co., VA	Medium-volatile bituminous